



# Blazars – The Observational Perspective

*An introduction gamma-ray observations of blazars*

Reshmi Mukherjee

2015 Fermi Summer School

# Outline

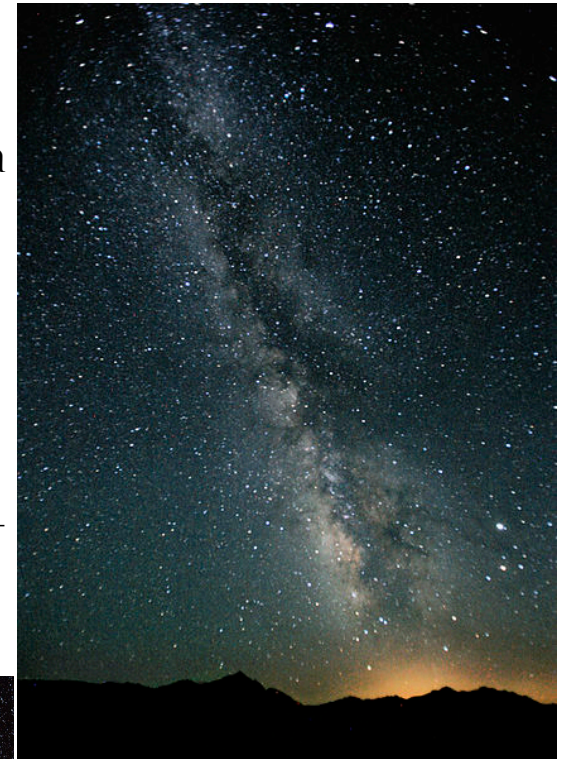
- I. Galaxies & active galaxies, AGN classifications, general introduction
- II. Blazar characteristics
- III. Production sites, acceleration & radiation mechanisms
- IV. Energy range & instruments
- V. GeV blazars
- VI. TeV blazars
- VII. GeV-TeV population studies
- VIII. Future prospects

- I. Galaxies & active galaxies, AGN classifications, general introduction

# Introduction: Galaxies & Active Galaxies

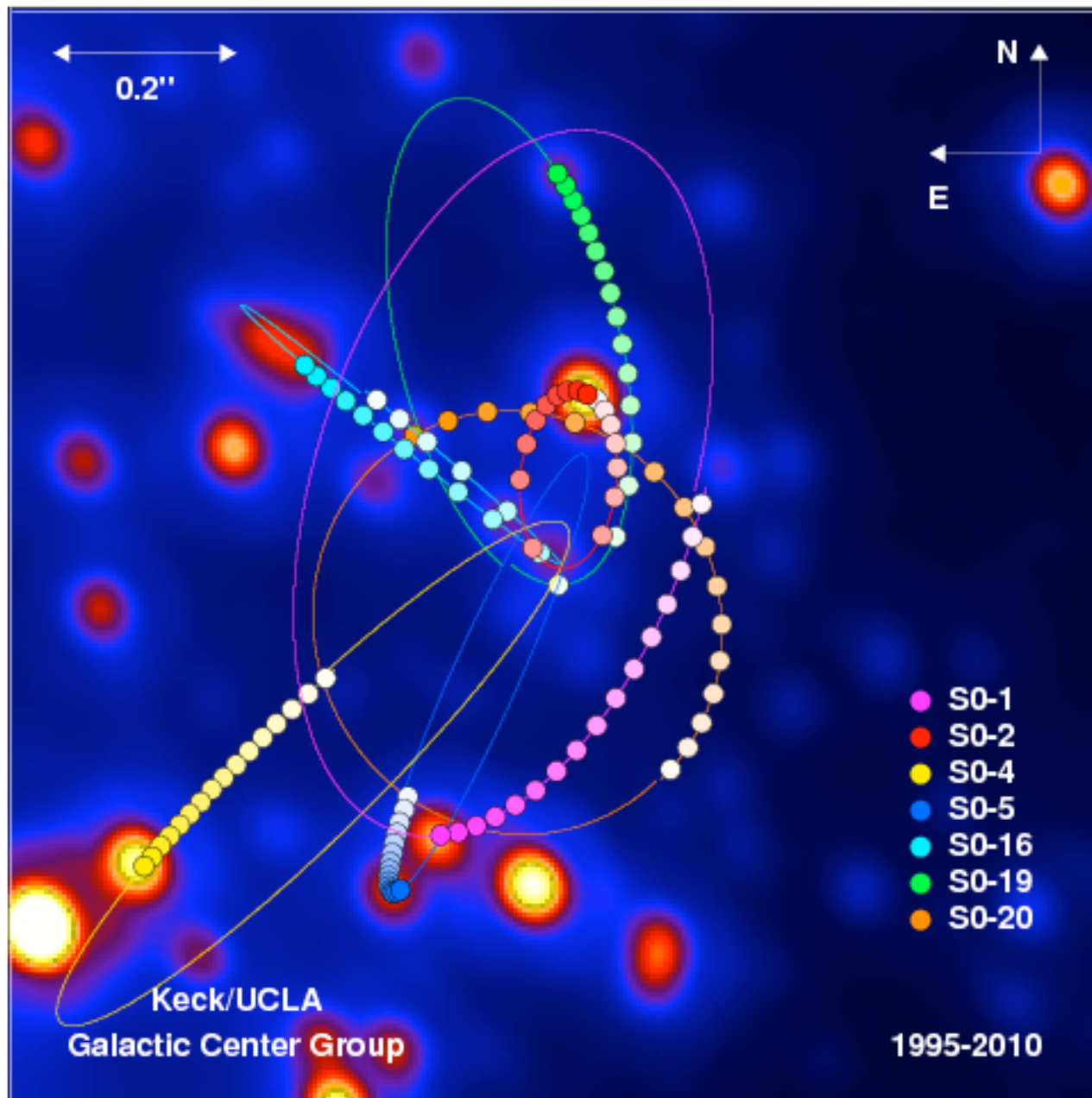
- The Universe is made up of galaxies, many containing more than hundred thousand million stars.
- The Milky Way galaxy (containing our solar system) is a barred spiral galaxy 100,000–120,000 light-years in diameter containing 200–400 billion stars.
- An **active galaxy** is a galaxy possessing an amazing power source at its nucleus – luminosity ~ thousands of MW galaxies.
- The power source in an active galaxy is very compact – approx. size of the solar system.
- We call these **Active Galactic Nuclei**

Andromeda Galaxy, our nearest neighbor spiral galaxy.

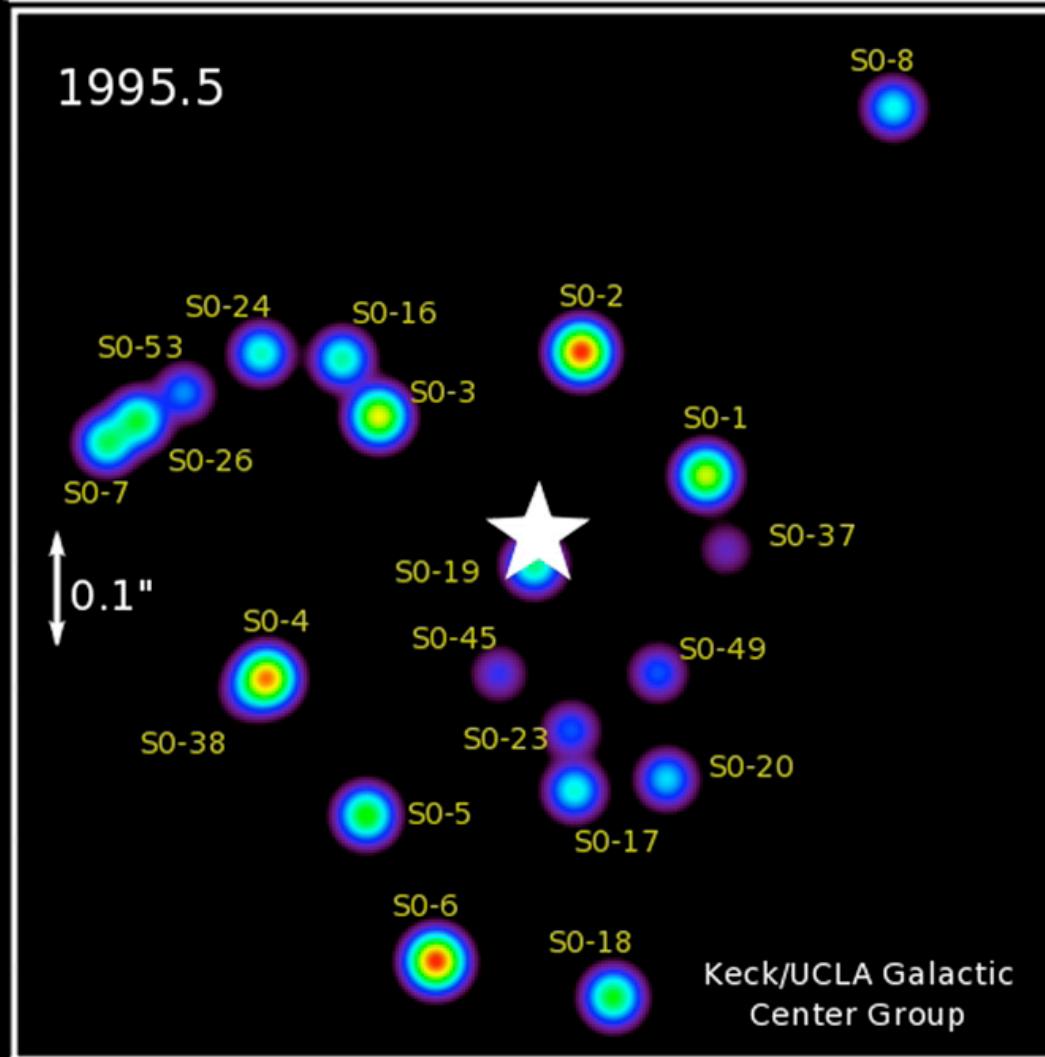


A view of the Milky Way towards the Constellation Sagittarius (including the Galactic Center) as seen from a non-light polluted area (the Black Rock Desert, Nevada).

# Stellar Orbits around the Galactic Center Black Hole

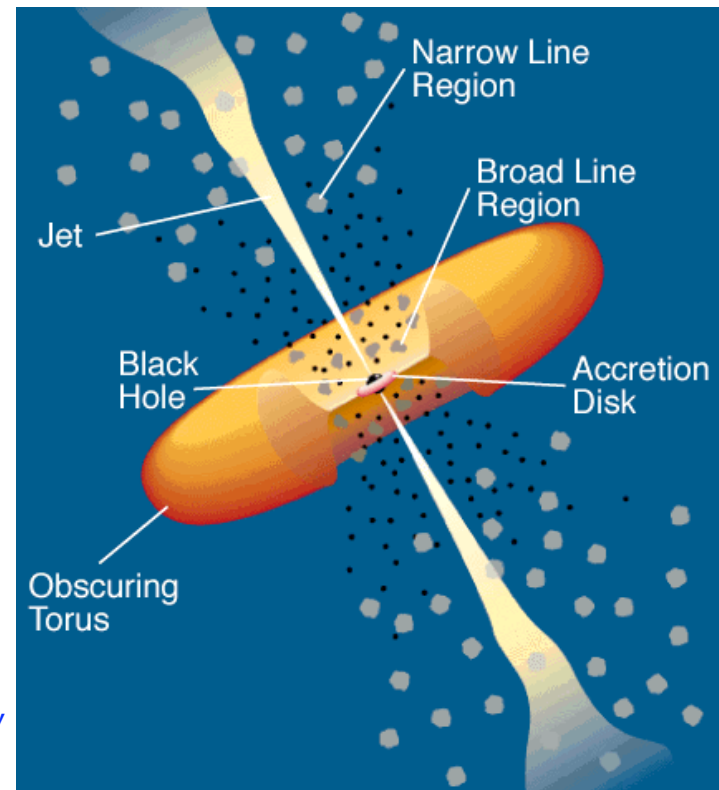


# Stellar Orbits: Galactic Center Black Hole



# Unified Model of AGN

- Extremely luminous objects
- Central luminosity outshines the light from all the surrounding stars of the host galaxy
- Emission (non-thermal) across entire spectrum ... radio to keV, MeV, TeV
- Relativistic jets, superluminal motion
- Current paradigm – blazars are powered by super-massive black holes (SMBH) located at or close to their centers  $\sim 10^9 M_{\odot}$  .



Urry & Padovani 1995

Schematic view of an AGN

Typical size of the galaxy is  $\sim 10^4$  pc. Central nucleus  $\sim 1-10$  pc.

# Unified Model of AGN

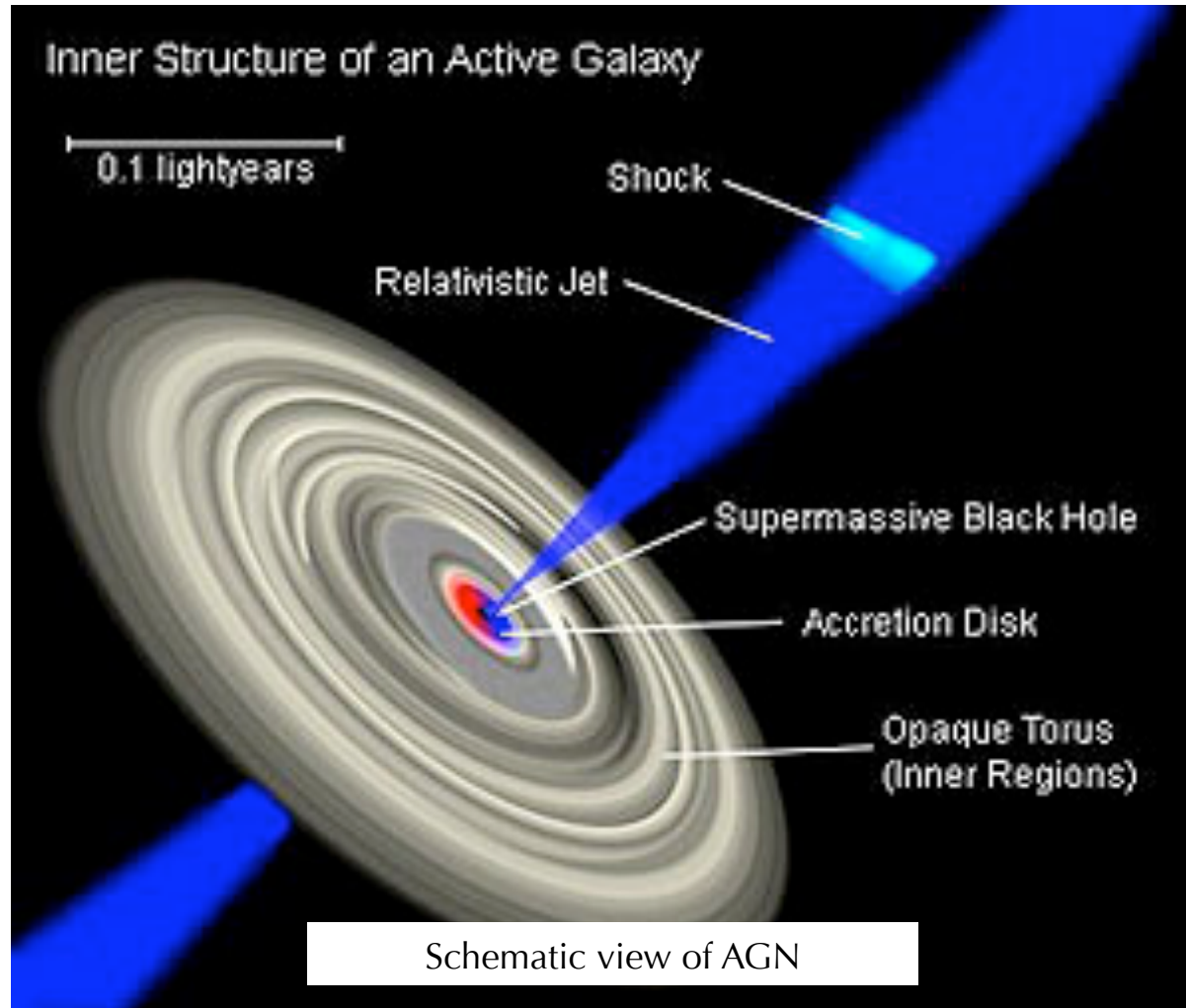


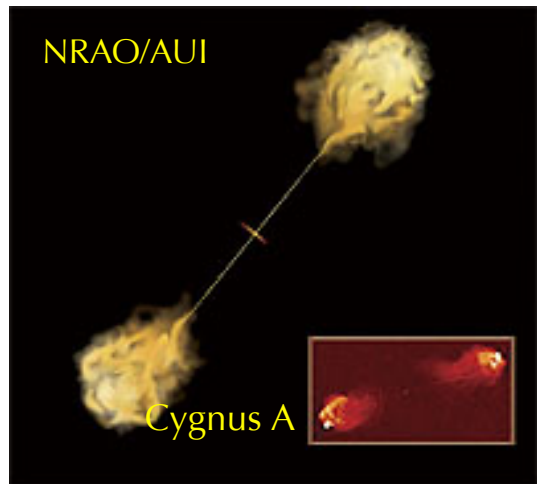
Image Credit: Galaxy Zoo

- The fundamental power source of active galaxies is the gravitational potential well of a SMBH.

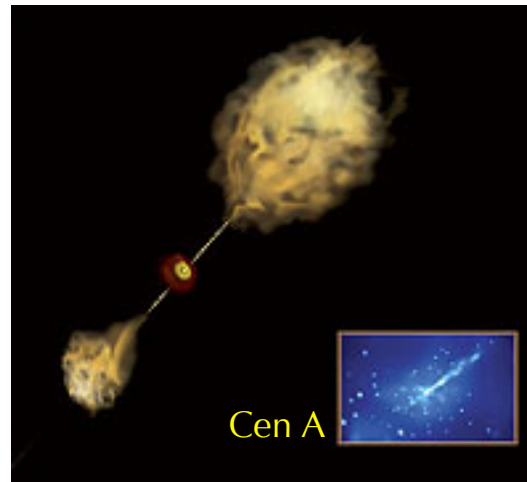


# What distinguishes the different types of AGN?

- the angle from which we happen to see it...

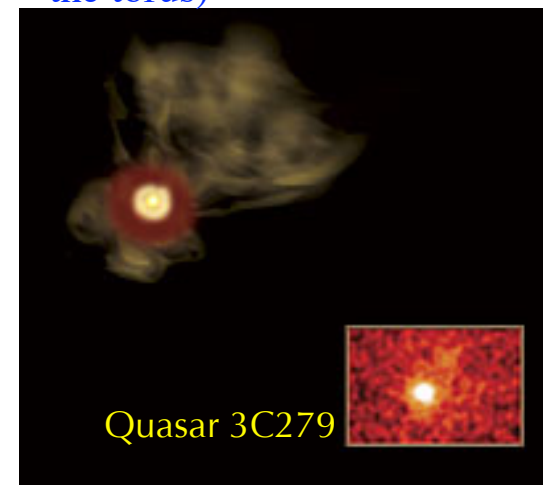


Looking edge-on, we would see a radio galaxy. (torus would block most of the radiation and all we'd see is the jet)



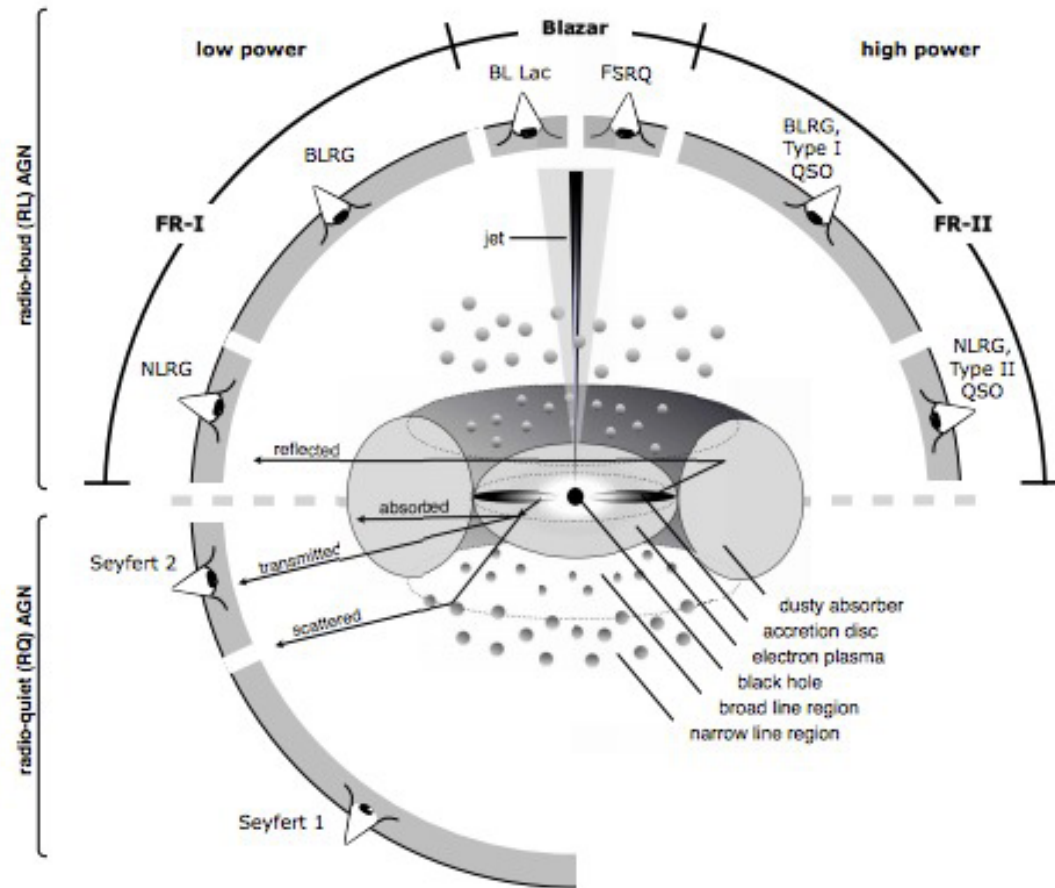
Looking at an angle, we would see a Seyfert Galaxy

Looking straight down the jet, we would see a blazar. (Emission from the jet would be so bright that it would swamp anything else from the accretion disk or the torus)



Images from Fermi/EPO

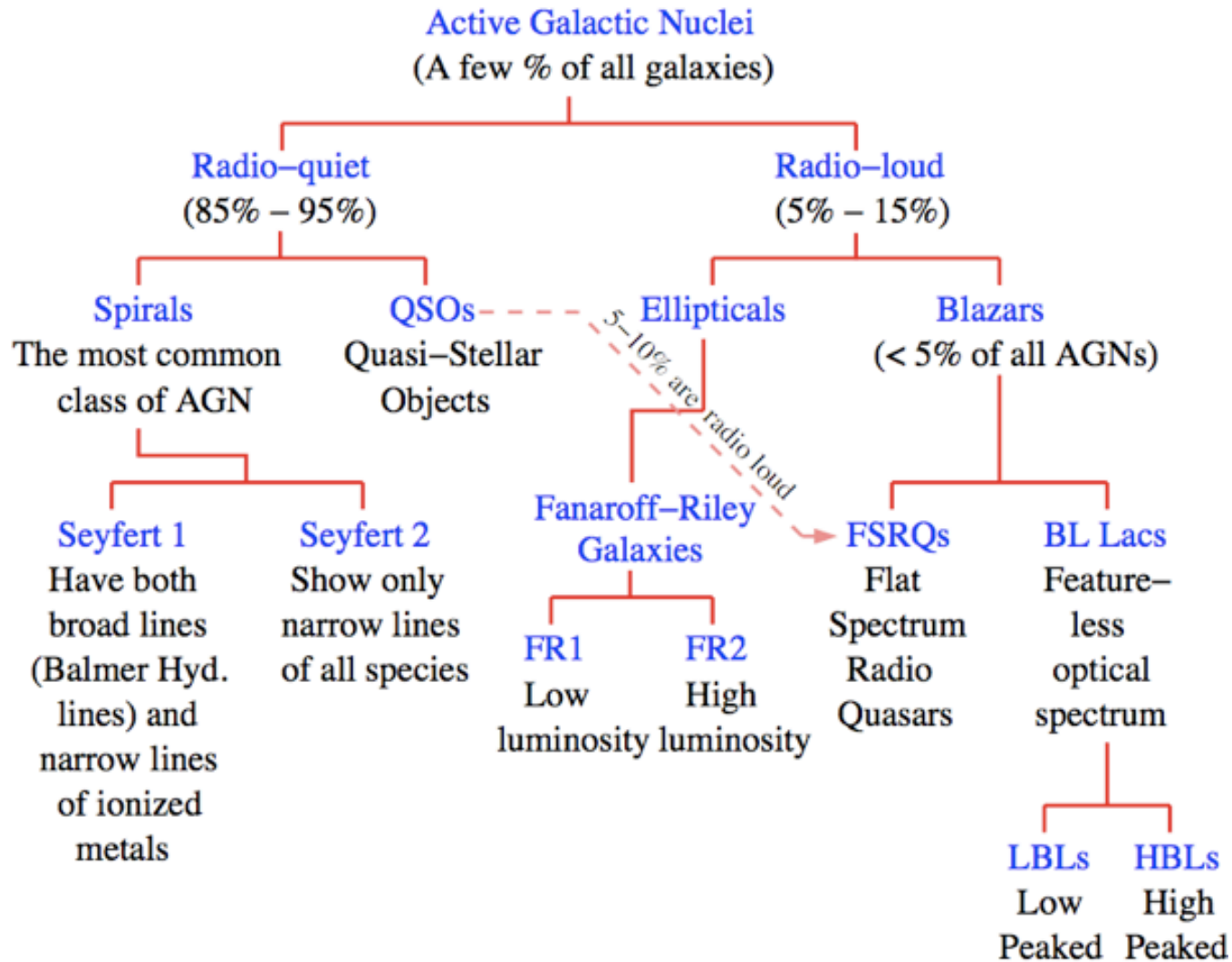
# What distinguishes the different types of AGN?



Beckmann & Shrader, astro-ph/1302.1397

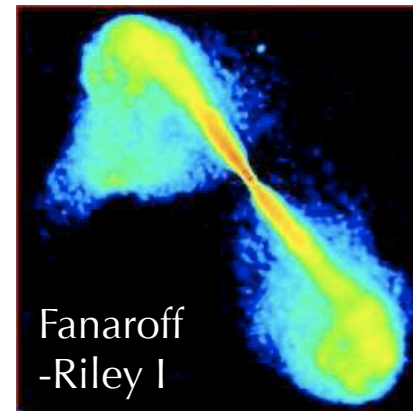
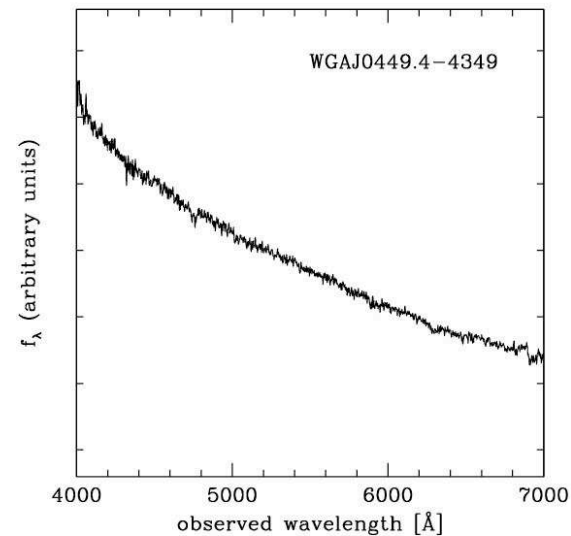
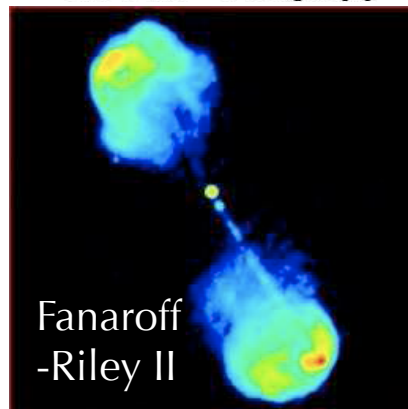
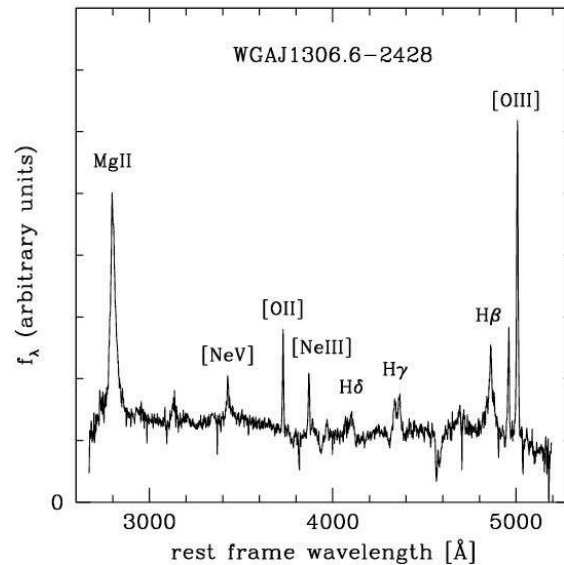
# AGN Classification

From D. Horan, Fermi School 2013



# Blazar Classes

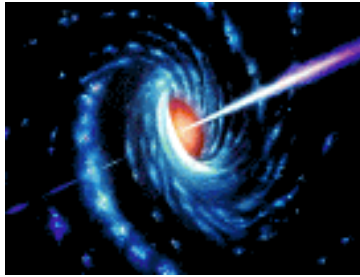
- Flat Spectrum Radio Quasar (strong broad lines)
- BL Lac: named after prototype BL Lacertae (weak or no broad lines)



See: "AGNs with the Fermi-LAT," B. Lott, [http://cta.obspm.fr/IMG/pdf/Atelier\\_CTA\\_2014\\_Lott.pdf](http://cta.obspm.fr/IMG/pdf/Atelier_CTA_2014_Lott.pdf)

## II. Blazar characteristics

# Blazars – General Characteristics



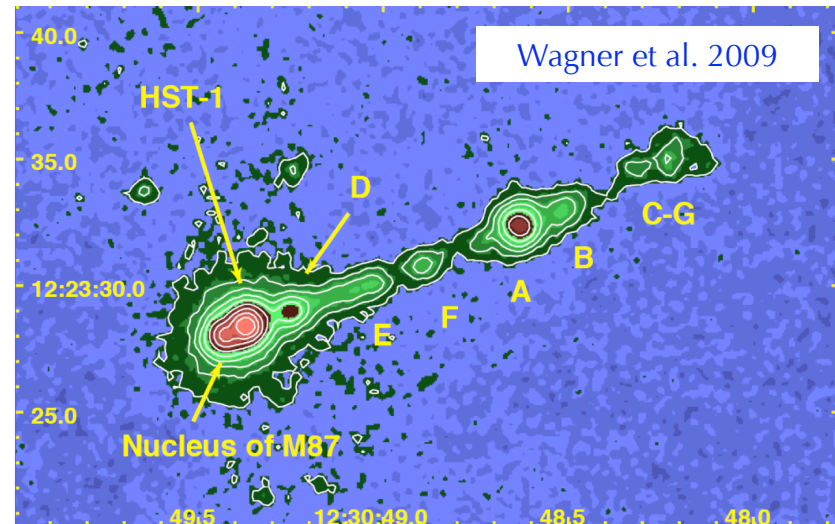
- Almost all AGN seen at high energies are *blazars* (BL Lacs & FSRQs):
  - Radio loud AGN viewed directly along the jet axis.
  - Flat spectrum radio sources ( $\alpha_r > -0.6$ ).

- FR Is are parent population of BL Lac objects
- FR IIs are parent population of FSRQs (Urry and Padovani 1995)
- **Blazars:** radio galaxies where jet is pointed towards us
- **Radio galaxies:** misaligned blazars

NASA/CXC/CfA/R.Kraft et al



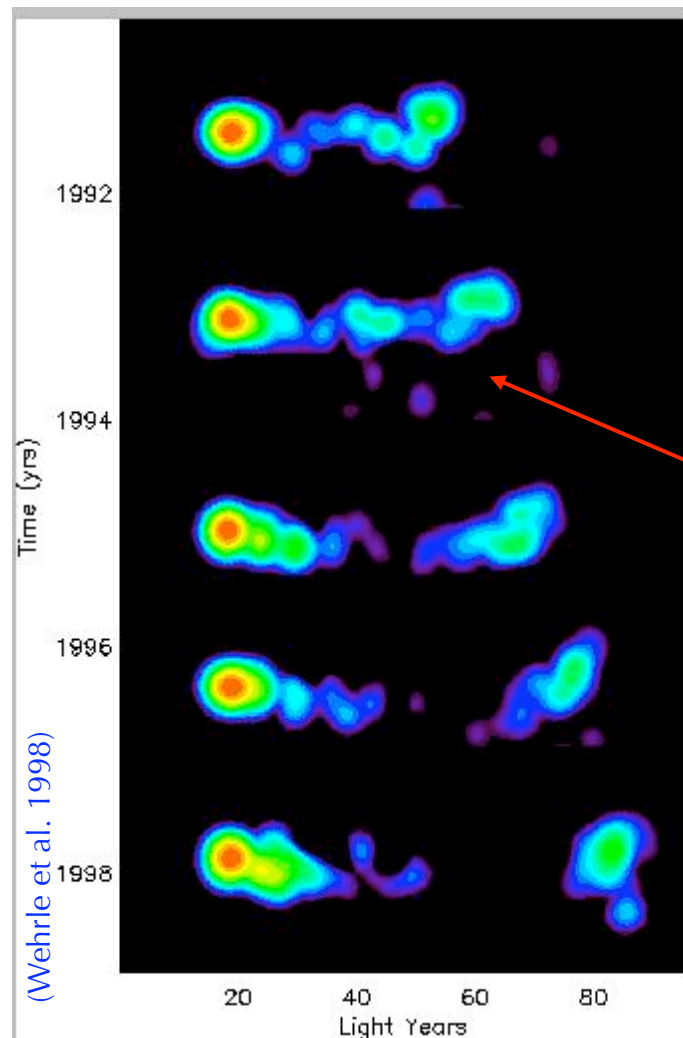
X-ray (Chandra) image of Cen A



X-ray (Chandra) image of the M87 jet

# Demonstrations of Relativistic Outflows

## Superluminal Motion in Blazars:



- High fraction of blazars are superluminal (evidence from VLBI)

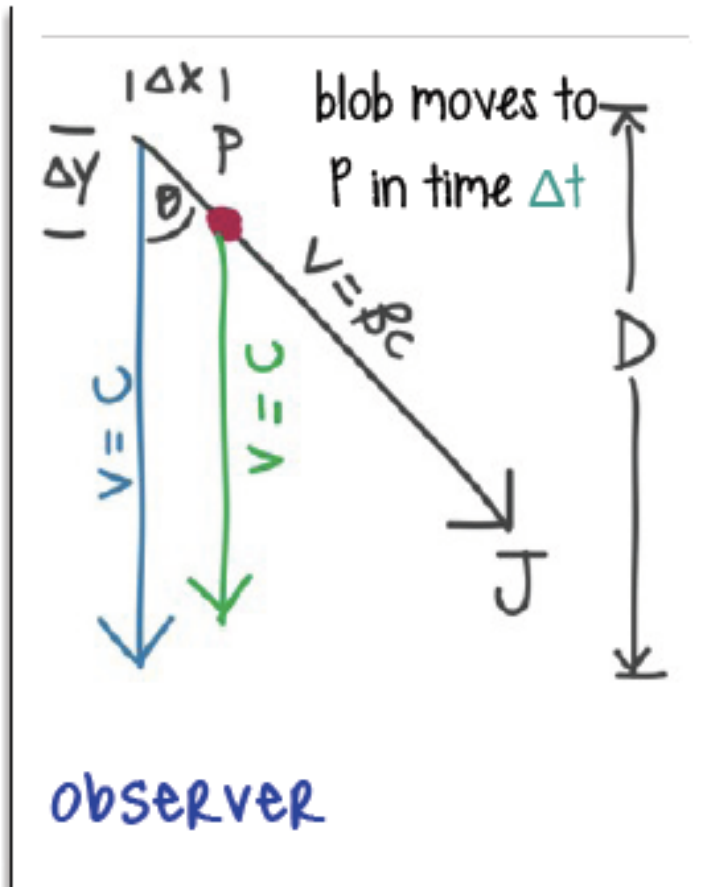
- Blobs move relativistically
- Trajectory inclined at small angles

Example: Long term high frequency VLBI monitoring of the relativistic jet in 3C 279 at 22 GHz. 1991 – 1997 (18 epochs)

- Bright, compact VLBI core and jet components. Apparent speeds measured for 6 super-luminal components  $\sim 4.8c - 7.5c$

# Blazars – Superluminal Motion

Superluminal motion: First proposed by Rees in 1966 (Nature, 211, 468) years before it was first observed when VLBI techniques were developed



- First pulse travels to observer in time  $D/c$
- Second, emitted time  $\Delta t$  later, has a shorter distance to travel:  $D - \Delta y$ .
- Velocity of observed blob separation on the plane of the sky:

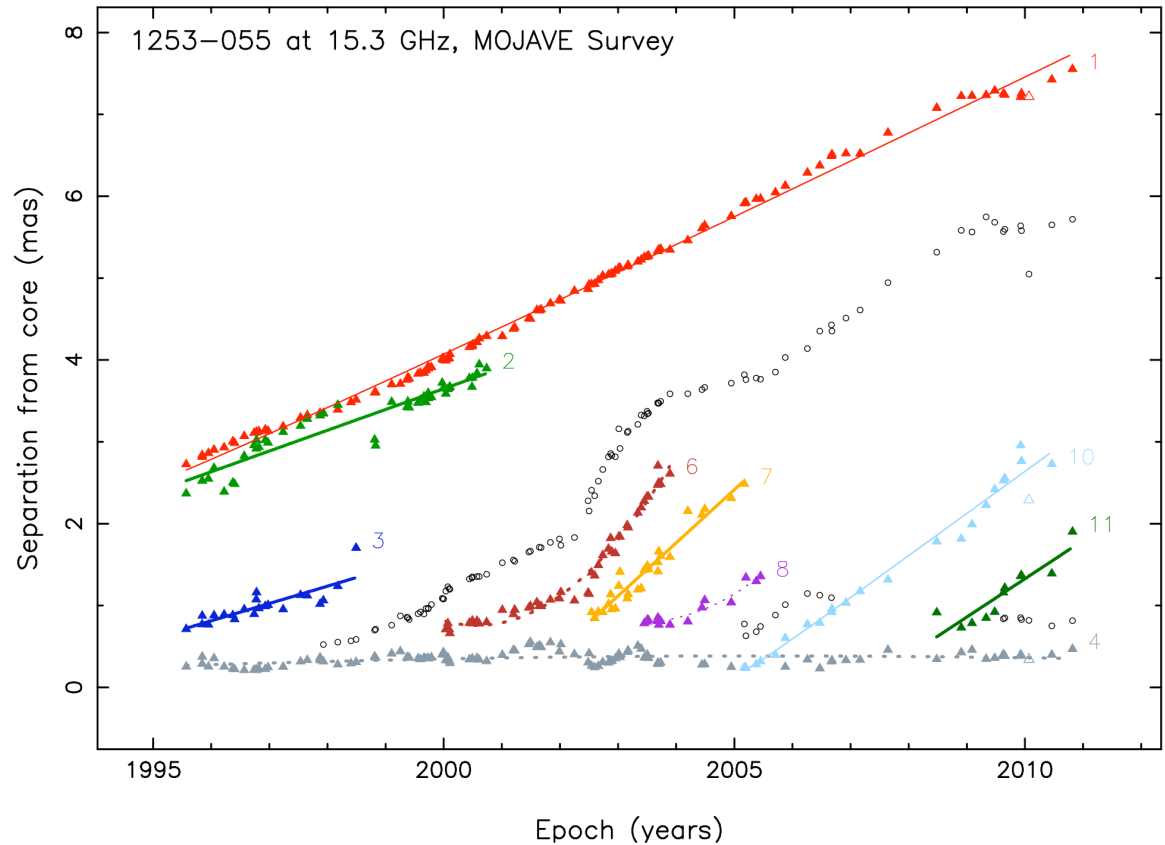
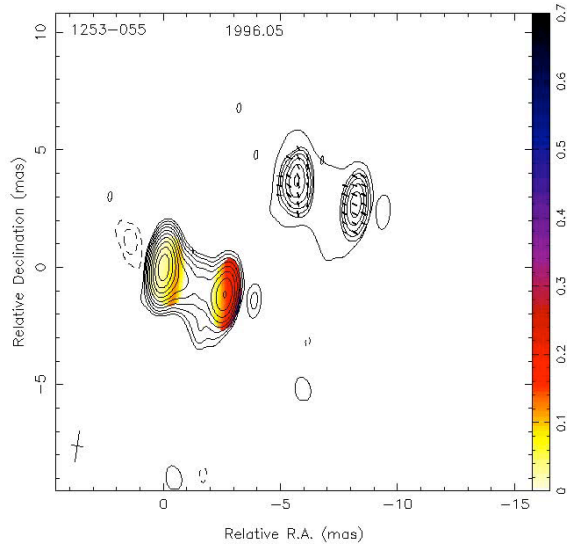
$$\beta_{\text{obs}} = \frac{\beta \sin \theta}{(1 - \beta \sin \theta)}$$

eg., for  $v \sim 0.99c$ ,  $\theta \sim 5^\circ$ ,  $\beta_{\text{obs}} \sim 6.27c$

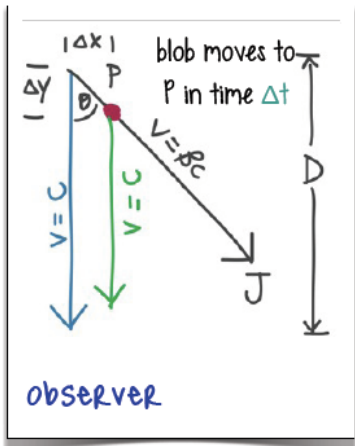
Figure from Deirdre HORAN --- 2013 Fermi Summer School --- Lewes, Delaware



# Superluminal Motion – MOJAVE Observations

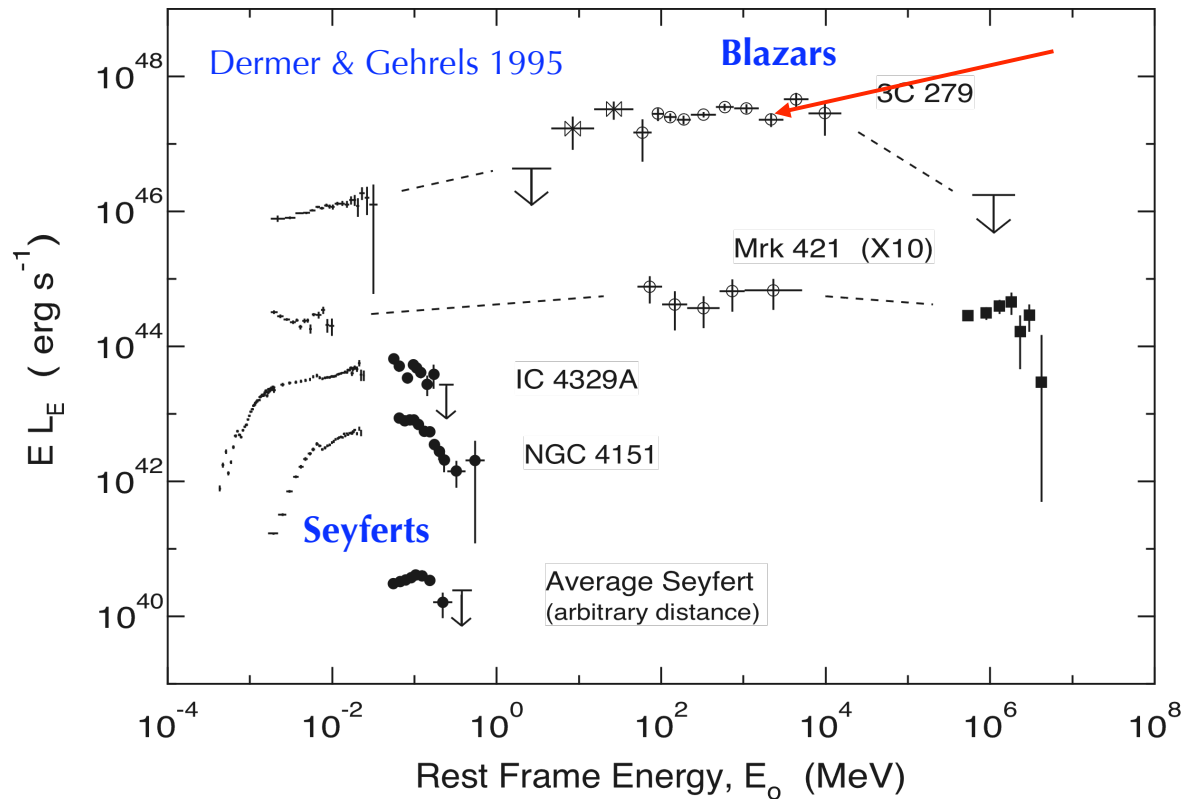


MOJAVE 2cm data. See:  
<http://www.physics.purdue.edu/MOJAVE/>



Apparent SL motion now seen from scores of radio sources, with apparent SL speeds typically between 1 and 10 (Vermeulen and Cohen 1994).

# Demonstrations of Relativistic Outflows



High isotropic  $\gamma$ -ray  
luminosity  $\sim 10^{48}$  erg/s

Non-thermal, continuum  
spectra. *Dramatic peak at  
 $\gamma$ -ray energies.* Emission  
extends to GeV-TeV  
band.

Absence of intrinsic  $\gamma\gamma$  pair absorption ---> beaming in blazars.

High luminosity  $\rightarrow$  optical depth  $\gg 1$ ,  $\gamma$ -ray emission originates in  
strongly beamed sources.

# Relativistic Beaming in Blazars

Two arguments for beaming:

## Absence of intrinsic $\gamma\gamma$ pair absorption

- Optical depth for  $\gamma\gamma \rightarrow e^+ e^-$  is proportional to **source compactness**:  $\frac{\sigma_T L}{4\pi c \langle E \rangle R}$
- For isotropic emission from a uniform spherical source at rest, and intrinsic  $L > 10^{48}$  erg/s  $\rightarrow$  optical depth  $\gg 1$
- Incompatible with the observed  $\gamma$ -ray spectra of the source

## Violation of the Elliot-Shapiro relation:

- For a spherically symmetric source in a steady state:  
 $L < L_{\text{Edd}} < 1.3 \times 10^{38} (M/M_{\odot})$  ergs/s.
- Min. intrinsic time scale of variation:  $\Delta t > R_s/c = 10^{-5} M/M_{\odot}$
- $\log \Delta t_{\text{obs}} / (1+z) > \log L_{48}$ . This condition is violated for several  $\gamma$ -ray blazars.

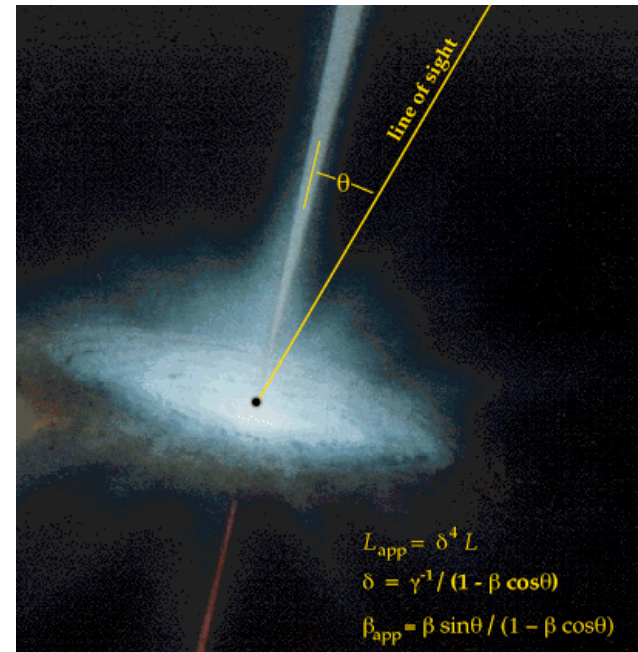
# Relativistic Effects in Blazars

- $\gamma$ -ray emission is NOT from isotropic sources at rest.
- Strong indication: Emission originates in sources moving at large bulk speeds towards us.
- Blazars are a useful laboratories for studying relativistic jets in AGN.
- Relate observed (\*) and intrinsic physical quantities (e.g. Rybicki & Lightman, 1979):
- Apparent Luminosity  $L_{\text{app}}^* = \delta^n L$ ,  $3 \leq n \leq 4$
- Doppler factor:  $\delta = [\Gamma(1 - \beta \cos \theta^*)]^{-1}$

$$\beta = V_{\text{jet}}/c$$

$$\Gamma = (1 - \beta^2)^{-1/2}$$

- Observers are particularly sensitive to blazars with small jet angles  $\Rightarrow$  Apparent Luminosity is Doppler boosted by a large factor.

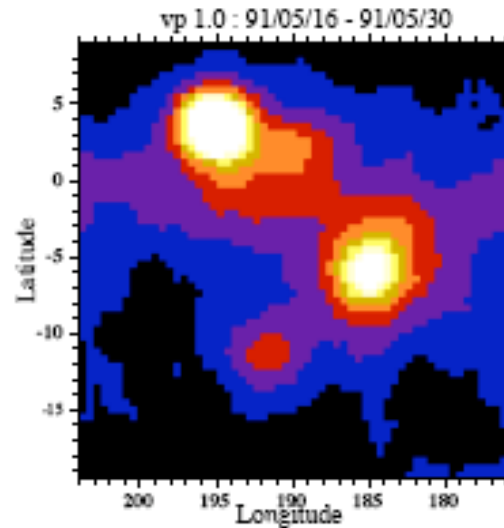
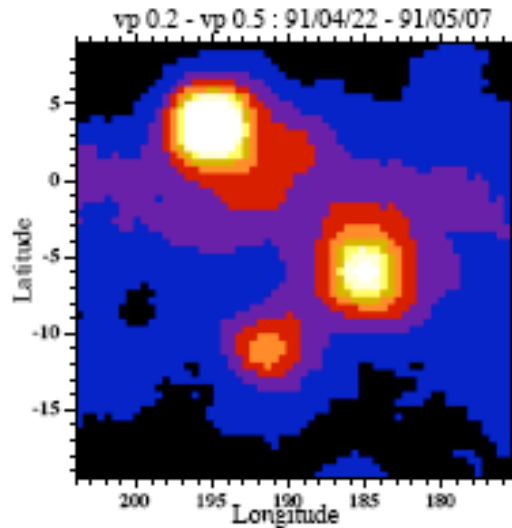


Observed emission  $S_{\text{obs}}$  is boosted in energy over that emitted in the rest frame S:

$$S_{\text{obs}} = S[\Gamma(1 - \beta \cos \theta)]^{-3}$$

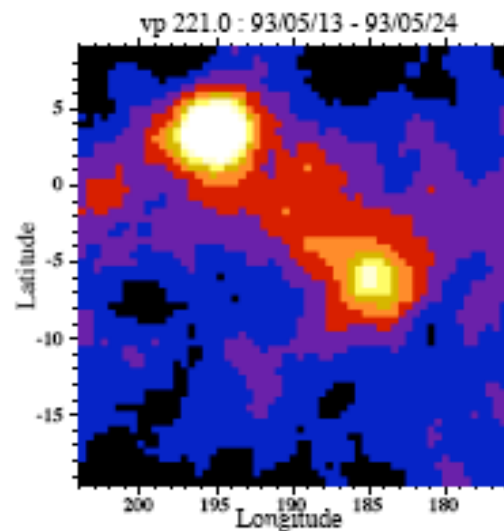
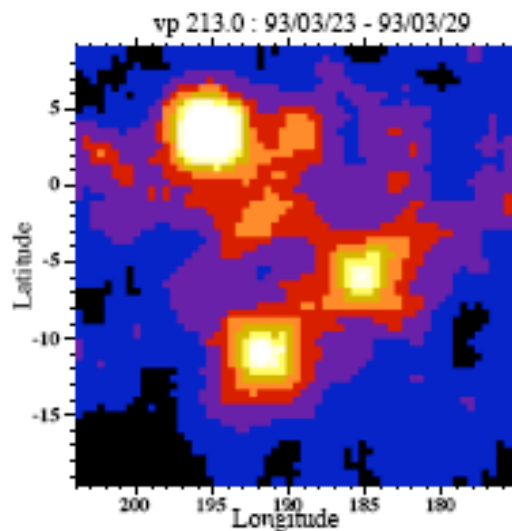
If plasma velocity is  $0.95c$  and  $\theta$  is  $5^\circ$ , boosting factor is  $\sim 200$

# Blazars – Variability



Strong time variability:

--> day-scale or less



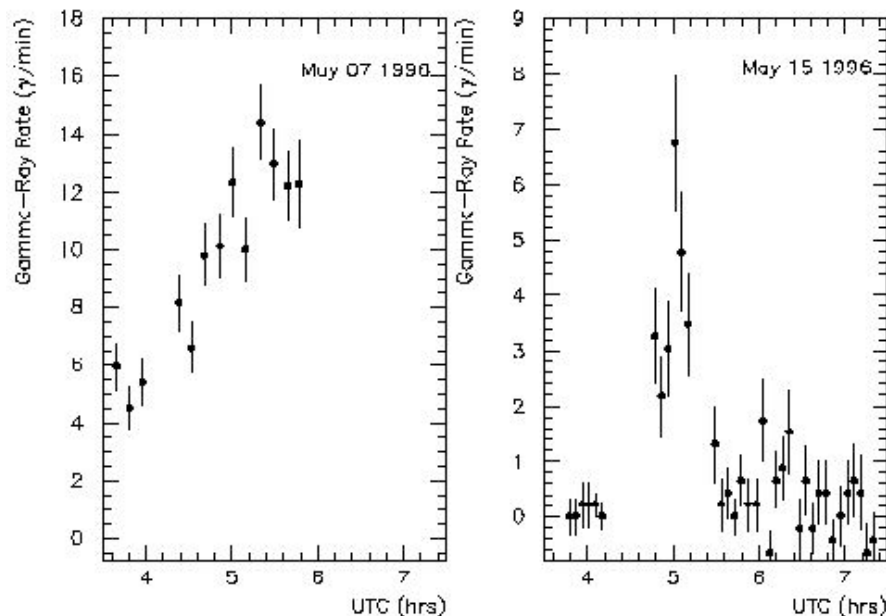
Old image of the Galactic Anti-Center from EGRET shows blazar [PKS 0528+134](#) flaring in gamma rays

# Light Curves

IACTs have the ability to study very short time scale variability in blazars.

Gaidos et al. 1995

Mrk421



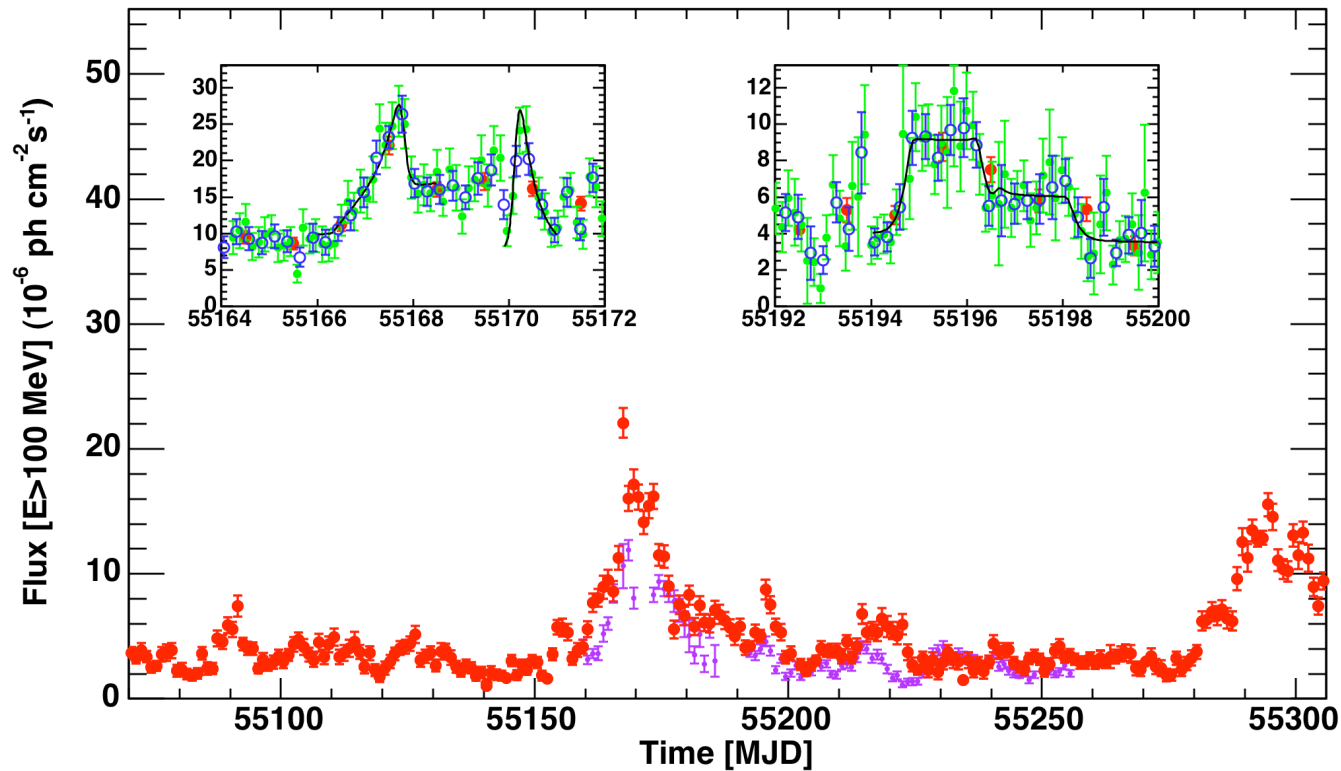
Variability timescale implies maximum emission region size scale.

- Rapid:  $< 15$  min var. time scale.
- Entire flare lasted  $\sim 30$  min.
- Fastest time scale variability seen in any blazar to date.
- ➔ compact emission region of  $\sim 1$ — $10$  light hours
- ➔ diameter –  $10$  Schwarzschild radius of a  $10^8$  solar mass black hole.

- $t_{\text{rise}} \approx t_{\text{fall}} \approx 15\text{min!}$
- $R < ct\delta/(1+z) \approx 10^{-4}\text{pc}$
- For  $M = 10^8 M_{\odot}$   $R_S \equiv 2GM/c^2 \approx 10^{-5}\text{pc}$

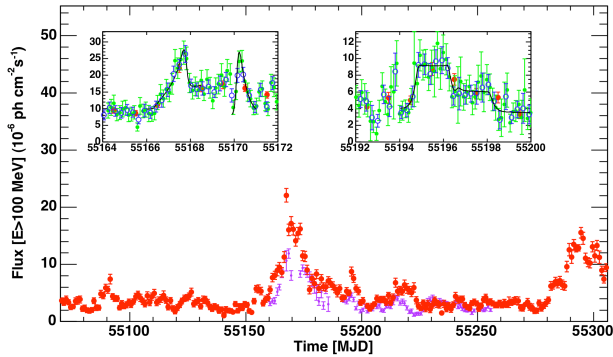
# Case Study: 3C 454.3 Light Curve

A minimum Doppler factor of 15 is derived, and the maximum energy of a photon from 3C 454.3 is 20 GeV



Ackerman et al. 2010, arXiv:1007.0483

# What can we say from the variability?



A photon flux of  $F_{E>100 \text{ MeV}} \sim 22 \times 10^{-6} \text{ ph cm}^{-2} \text{ s}^{-1}$  from 3C 454.3 at  $z = 0.859$  implies an apparent isotropic  $\gamma$ -ray luminosity above 100 MeV of  $L_\gamma \sim 3.3 \times 10^{49} \text{ erg s}^{-1}$ .

Estimates for the black-hole mass in 3C 454.3 range from  $M_9 \approx 1$  (Bonnoli et al. 2010) to  $M_9 \approx 4$  (Gu et al. 2001).

To be radiating below the Eddington luminosity of  $1.26 \times 10^{47} (M_9 M_\odot) \text{ erg s}^{-1}$  for a  $10^9 M_9$  Solar mass black hole implies that the high-energy radiation is beamed into a jet with opening angle  $\theta < 0.1$

A minimum Doppler factor of 15 is derived, and the maximum energy of a photon from 3C 454.3 is 20 GeV

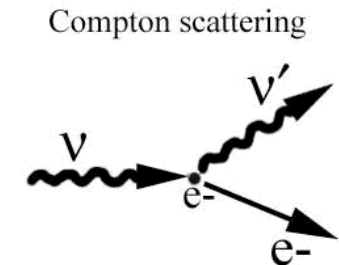
$$\delta_{min} \simeq \left[ \frac{\sigma_T d_L^2 (1+z)^2 f_{\epsilon} \epsilon_1}{4 t_{var} m_e c^4} \right]^{1/6} \quad \delta_{min} < \delta \equiv [\Gamma(1 - \beta \cos \theta)]^{-1},$$



### III. Gamma-ray production site, acceleration and radiation mechanisms

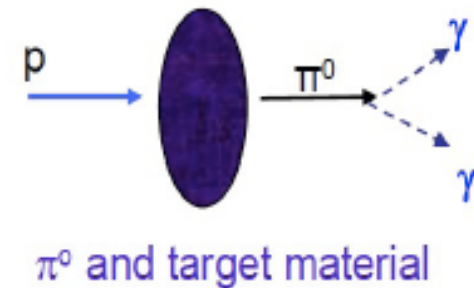
# How are gamma-rays produced?

- charged particles get accelerated
  - shock
  - pulsar B
- electrons
  - emit synchrotron radiation (X-rays)
  - inverse-Compton scatter ambient photons to VHE
  - double-hump feature in extended spectra
- protons
  - collide with ambient gas (beam-dumps)
  - $\pi_0 \rightarrow \gamma\gamma$

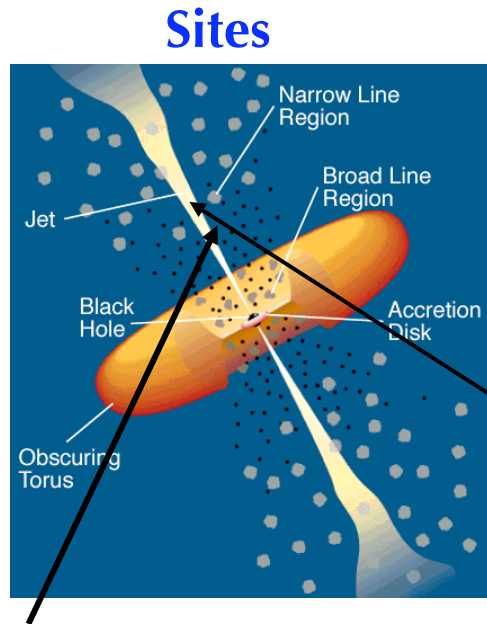


$$\nu' < \nu$$

Electron is initially at rest  
 $e^-$  gains energy



# Physics of Blazars



Jet powered by accretion of matter onto SMBH.

Unfortunately, we cannot image AGN in  $\gamma$  rays. Hence, physics of blazars may only be inferred through energy and spectral variability studies.

## Acceleration

- relativistic shocks
- stochastic (Fermi II) accel.
- magnetic reconnection
- plus complex magnetohydrodynamics

Ultrarelativistic particles (GeV/TeV) injected into blob

## Radiation

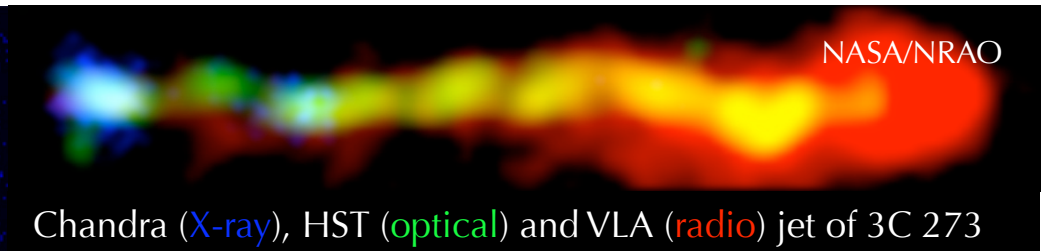
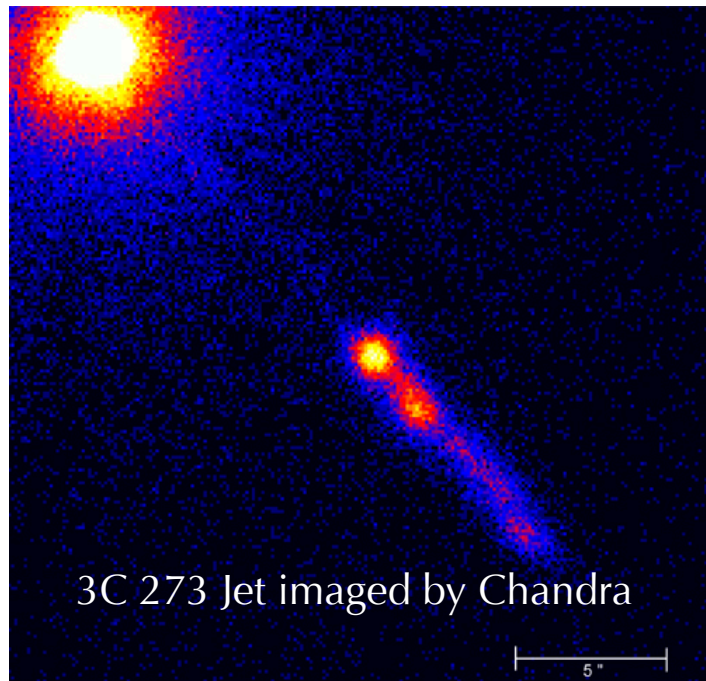
- Inverse Compton
- Electron synchrotron
- Proton synchrotron
- Photomeson processes (and subsequent pair cascades  $\gamma\gamma$  pair production)

## Current Paradigm

- Synchrotron self Compton
- External Compton
- Proton induced cascades
- Proton synchrotron

# Production Sites: Blazar Jets

Relativistic jets directed towards the observer

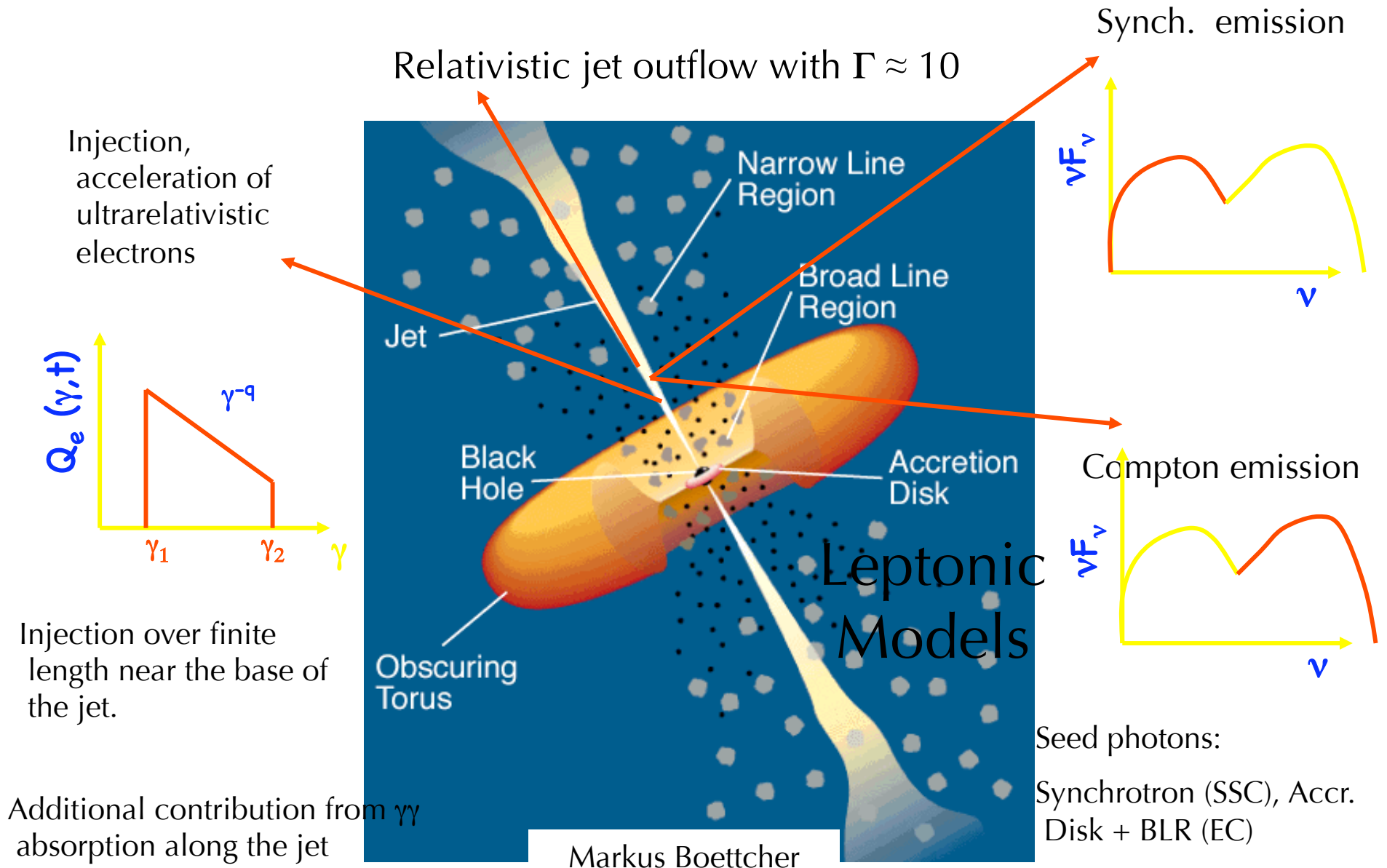


- Jet is approximately 20 arc sec  
(1 arcsec = 3 kpc ( $z = 0.158$ ,  $H_0 = 65$  km/s Mpc))

From radio to X-rays, non-thermal emission is observed. Gamma rays expected in all scales from sub-pc to multi-kpc scales.

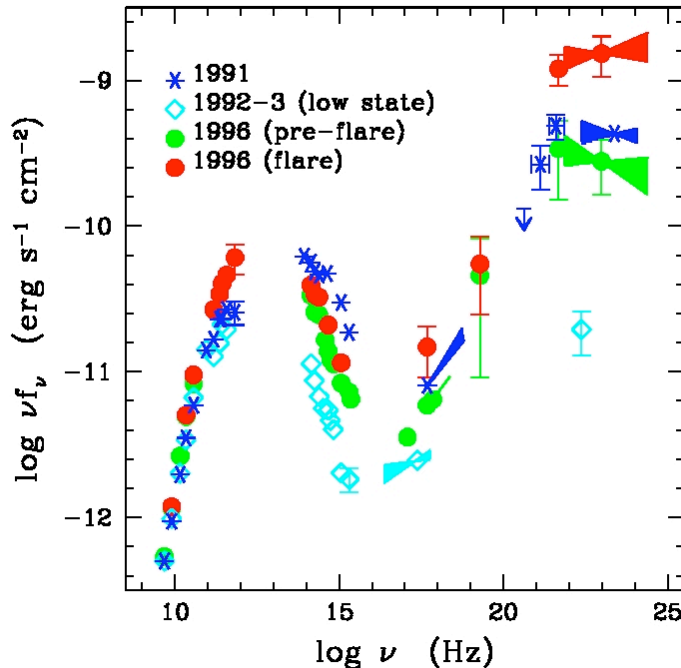
High energy (GeV) and VHE (TeV)  $\gamma$  rays have been detected from large numbers of AGN

# Blazar Models

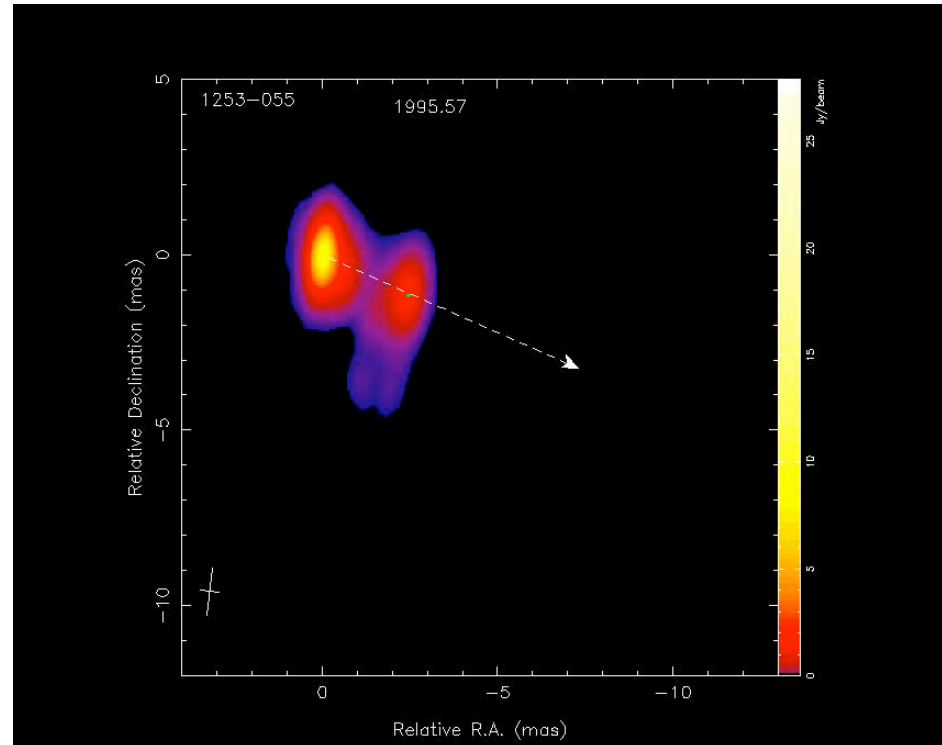


# Types of Blazars: Flat-spectrum Radio Quasar

Multi-epoch SED of 3C 279



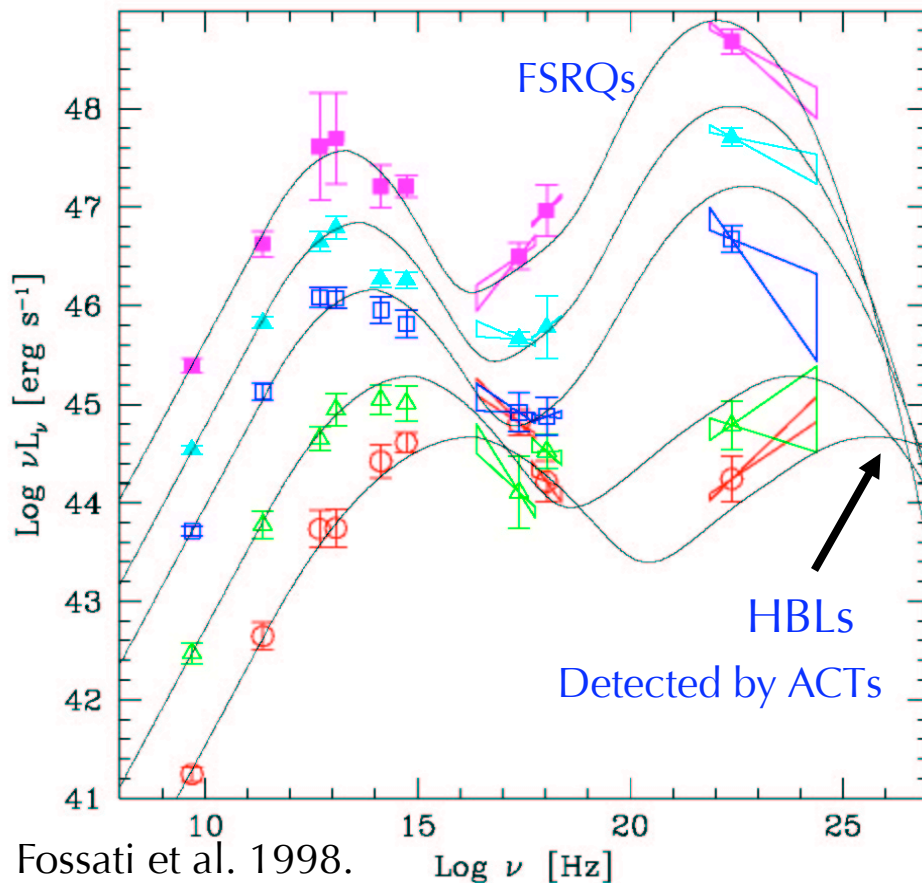
Wehrle et al. (1998) / MOJAVE



Maximum jet speed:  $651 \pm 25 \mu\text{s/y}$  ;  $20.58 c$   
(based on 9 moving features, Lister et al. 2013)

- Highly luminous sources. High energy component dominates.
- Optical spectrum shows prominent broad emission lines. Big blue bump often present.
- Typically extremely variable optical continuum ("Optically violently variable quasars")
- "Knotty" parsec-scale jets

# Understanding SEDs of Blazars

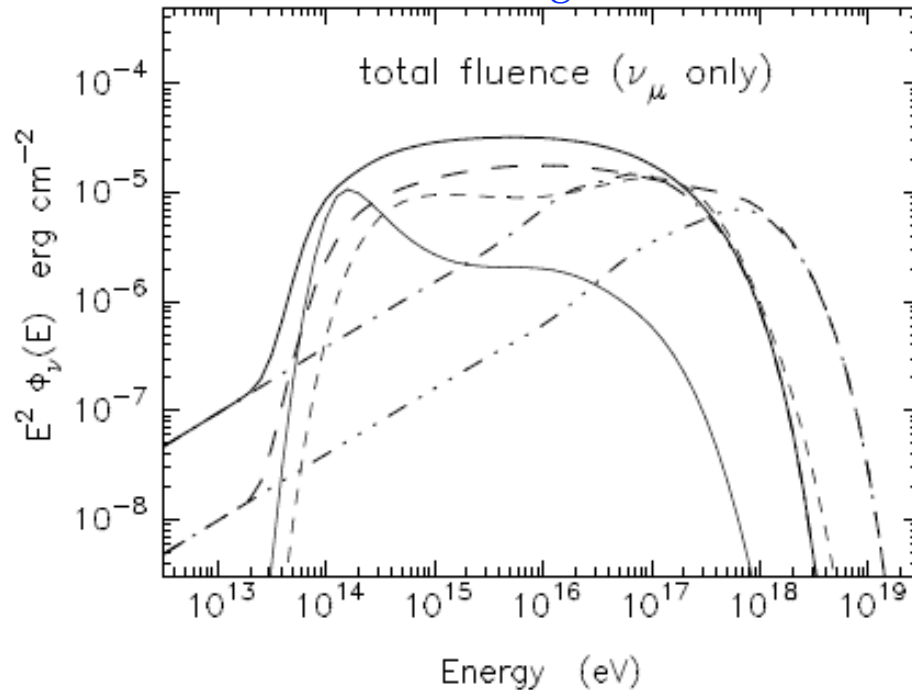


- Non-thermal emission consists of at least 2 distinct, broad spectral components.
- Sequence of sub-classes of blazars defined through the peak frequencies and the relative power of those components.
- ~~No FSRQs detected by ACTs at  $> 100 \text{ GeV}$ .~~

The lack of sufficient number of GeV-TeV blazars limits our understanding of the  $\gamma$ -ray emission, and our ability to extrapolate results to the larger population of radio sources

# Neutrinos ?

Fluences of neutrinos integrated over several days.



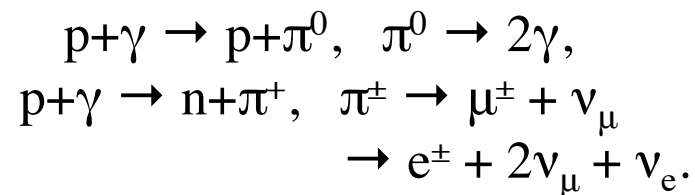
Atoyan & Dermer (2004)

*For hadronic models:*

- HE neutrinos expected (e.g. Gaisser et al. 1995).
- Fluxes of multi-TeV  $\nu$  should be seen by km-scale detectors like IceCube.
- Powerful blazars with strong accretion-disk radiation are good candidates.
- **Observation of  $\nu$  would be direct proof of hadron accel. in AGN jets.**

▪ **Nuclear interaction with ambient jet matter:**  $p + p \rightarrow \pi^{\pm,0} \rightarrow \nu, e^\pm, \gamma$

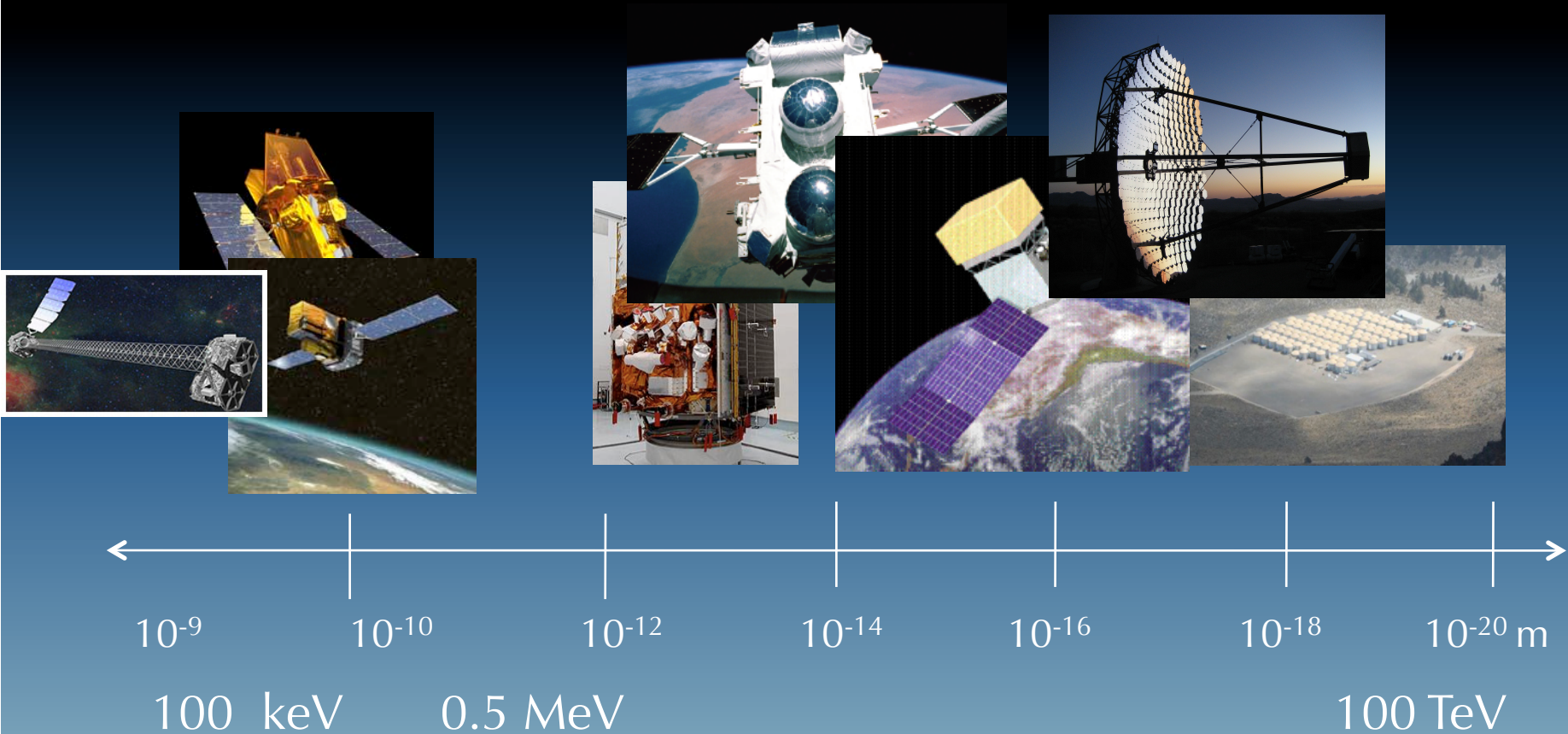
▪ **Photomeson interactions:**





## IV. Energy Range & Instruments

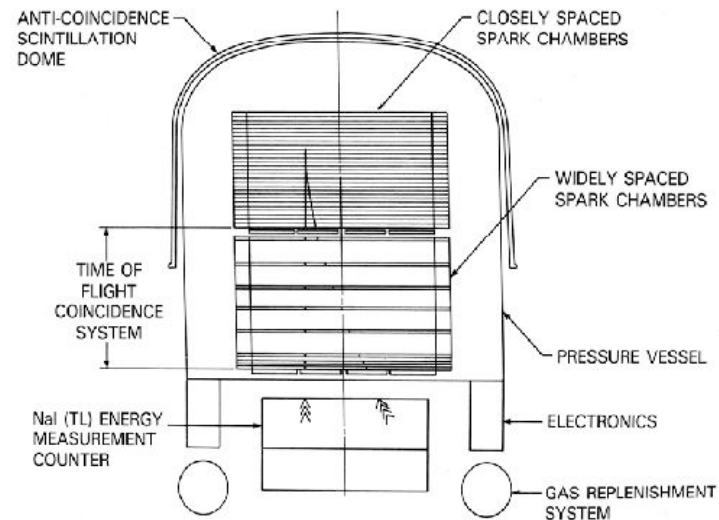
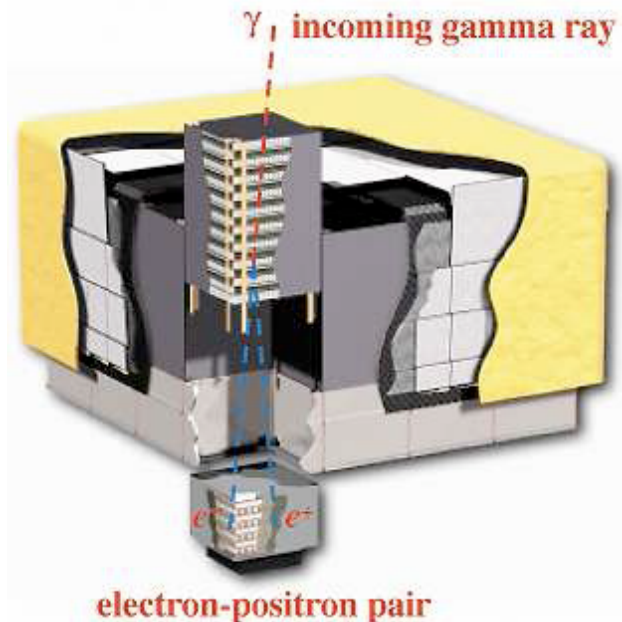
# High Energy Instruments



## V. GeV Blazars

# Fermi-LAT & EGRET (CGRO)

Gamma-ray telescopes image one photon at a time



Launched 2008. Mission lifetime 5y, goal 10y of operations (no consumable on board).

Energy range: 20 MeV - 300 GeV

- Catalog: 1FGL, 2FGL, 3FGL....
- AGN catalog: 3LAC
- 3000 sources in 3FGL
- 1563 AGN at  $b > 10^0$ . 98% blazars

EGRET: Energetic Gamma Ray Experiment Telescope

In orbit: 1991 – 2000

Energy range: 20 MeV to 30 GeV

- Catalog: 3EG....
- 94 sources in 3EG
- 56 FSRQs
- 14 BL Lacs

# Blazar Skymap & Spectrum

period covered by the EGRET observations, the high-energy flux from PKS 0528+134 varied over the range  $(2.3 \pm 1.2 \text{ to } 30.8 \pm 3.5) \times 10^{-7}$  photons  $\text{cm}^2 \text{s}^{-1}$ . Table 1 lists the measured flux and the flux upper limit for each of the viewing periods in which PKS 0528+134 was in the EGRET FOV. The highest flux from PKS 0528+134 was detected in viewing period 213.0, when it was greater by a factor of about 2 compared to the highest flux reported earlier by Hunter et al. (1993). A  $\chi^2$  test of the data yields a probability of less than  $10^{-5\%}$  that the fluctuations are consistent with a constant flux.

In order to study variability over shorter timescales, VP 213.0, during which PKS 0528+134 was observed in the "high" state, was broken up into four intervals each of length 1.425 days. The average flux was calculated for the four time ranges. The results are shown in Figure 1b. The flux appears to decrease sharply after an initial steady increase during the first three quarters of the viewing period. The data points have large error bars, and a  $\chi^2$  test indicates that there is about a 15% probability that the fluctuations are consistent with a constant flux.

## 2.2. Spectrum

In order to determine the background-subtracted high-energy gamma-ray spectrum of PKS 0528+134, the energy range 30 MeV–10 GeV was divided into 10 energy intervals, and maps of photons and exposures were made for each of the energy ranges. Likelihood analysis was used to estimate the number of source photons in each of the 10 energy bins. Due to EGRET's finite energy resolution and its nonuniform detection efficiency over the energy range, the observed spectrum of the source differs from its true spectrum. The data were fit to a single power-law model, following the general approach used in EGRET data analysis (Nolan et al. 1993; Fichtel et al. 1993; Hughes & Nolan 1989). The form of the model used was

$$F(E) = k(E/E_0)^{-\alpha} \text{ photons cm}^{-2} \text{ s}^{-1} \text{ MeV}^{-1}, \quad (1)$$

where the photon spectral index,  $\alpha$ , and the coefficient,  $k$ , are the free parameters. The energy normalization factor,  $E_0$ , was chosen so that the statistical errors in the power law index and the overall normalization were minimally correlated.

Figure 2 shows the photon spectrum of PKS 0528+134 as observed during VP 213.0 when the source was in the "high" state. The best fit using equation (1) is shown as a superimposed solid line in the figure. The best-fit parameters are indicated in Table 2. The errors in the fit parameters correspond to  $1 \sigma$  uncertainties and are statistical only. The systematic errors in the EGRET measurements are typically smaller than the statistical errors (Thompson

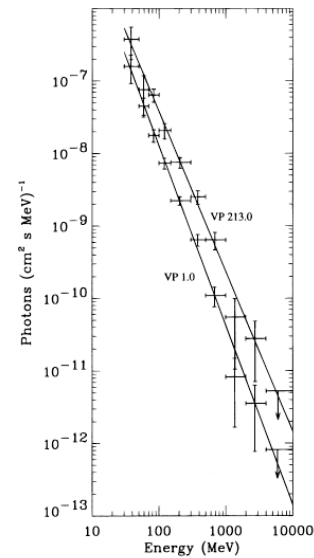
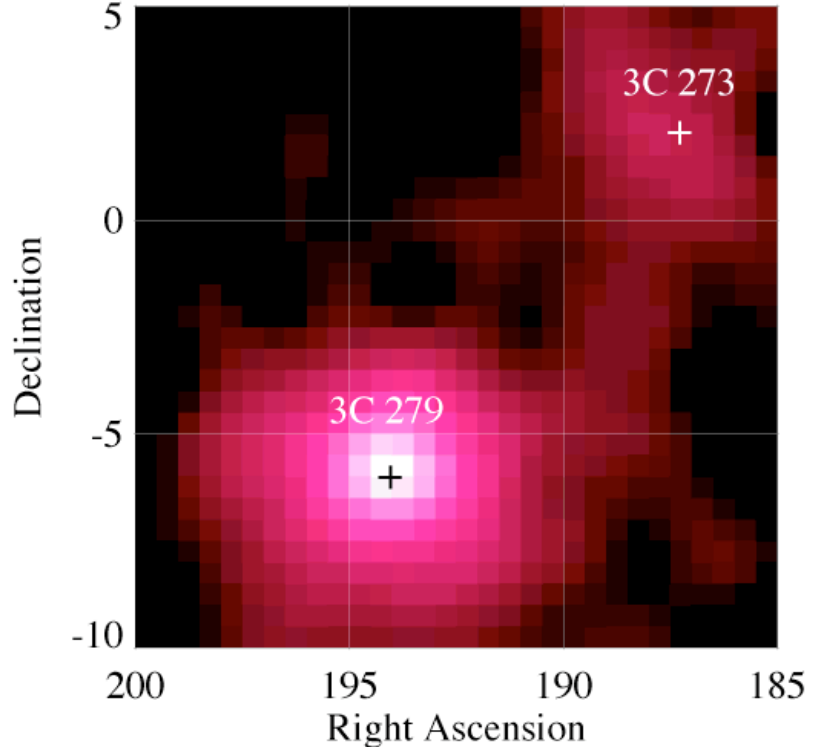


FIG. 2.—Photon spectra of PKS 0528+134 as observed during VP 1.0 and VP 213.0, when the source was in an outburst. Solid lines are the best fits to the power law shown in eq. (1).

et al. 1993) and have been neglected here. The reduced  $\chi^2$  of the fit is 0.78, indicating an adequate fit.

The photon spectral index of PKS 0528+134,  $\alpha = 2.48 \pm 0.09$ , for the observations made in VP 1.0 is much steeper than the value of  $2.21 \pm 0.10$  obtained for VP 213.0. For comparison, Figure 2 also shows the spectrum for VP 1.0. The superimposed line corresponds to the best fit using equation (1), with a reduced  $\chi^2$  of 0.83. The best-fit parameters are given in Table 2. These results suggest that there is a tendency for spectral hardening when the source is in an outburst. PKS 0528+134 was also detected with high statistical significance during 1991 April, in VP 0.2, 0.3, 0.4, and 0.5. The observed flux during this time was higher than that observed in VP 1.0, but much lower than that in VP 213.0. A spectral analysis of the data for the combined viewing periods 0.2, 0.3, 0.4, and 0.5, yields a photon spectral index of  $\alpha = 2.27 \pm 0.07$ . The results of the spectral analysis are tabulated in Table 2.

Figure 3 shows a plot of the photon spectral index versus the measured flux for photon energies greater than 100 MeV for PKS 0528+134. Viewing periods in which the source was in a low flux state were added together for spectral analysis and is shown as "Sum" in Figure 3 and Table 2. The data indicate that there appears to be a marginal correlation between the spectral index and the measured



Data from EGRET

Viewing Period	Spectral Index ( $\alpha$ )	$k \times 10^{-9}$ (photons $\text{cm}^{-2} \text{s}^{-1} \text{ MeV}^{-1}$ )	$E_0$ (MeV)	$\chi^2/n_f$
0.2–0.5.....	$2.27 \pm 0.07$	$3.26 \pm 0.19$	199	1.53
1.0.....	$2.48 \pm 0.09$	$3.33 \pm 0.26$	172	0.83
213.0.....	$2.21 \pm 0.10$	$8.39 \pm 0.77$	198	0.78
Sum.....	$2.56 \pm 0.17$	$1.87 \pm 0.20$	150	0.56

\* Sum of viewing periods 2.1, 36.0, 36.5, 39.0, 310.0, 321.1, 321.5, and 337.

# We've come a long way....

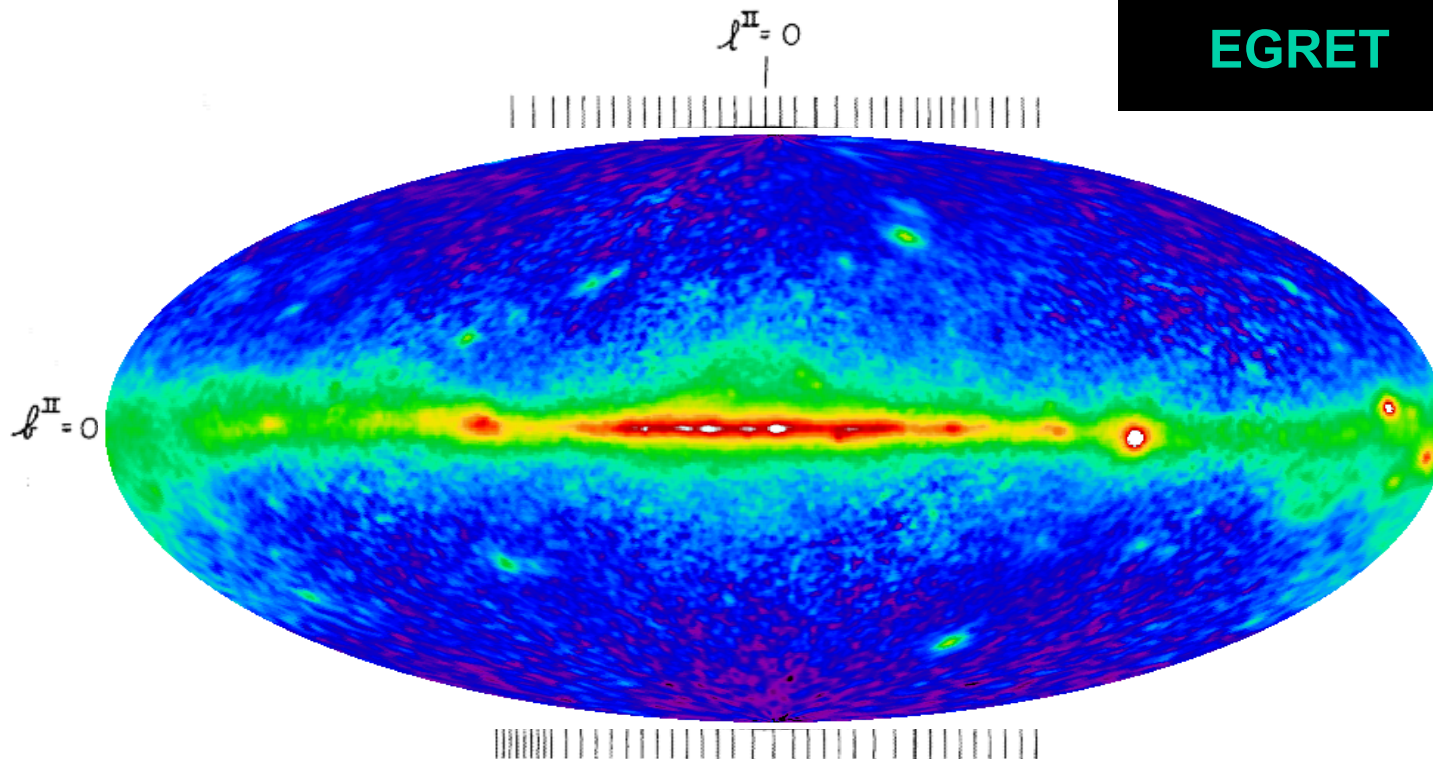
(slide from S. Digel)

356

W. L. KRAUSHAAR *ET AL.*

Vol. 177

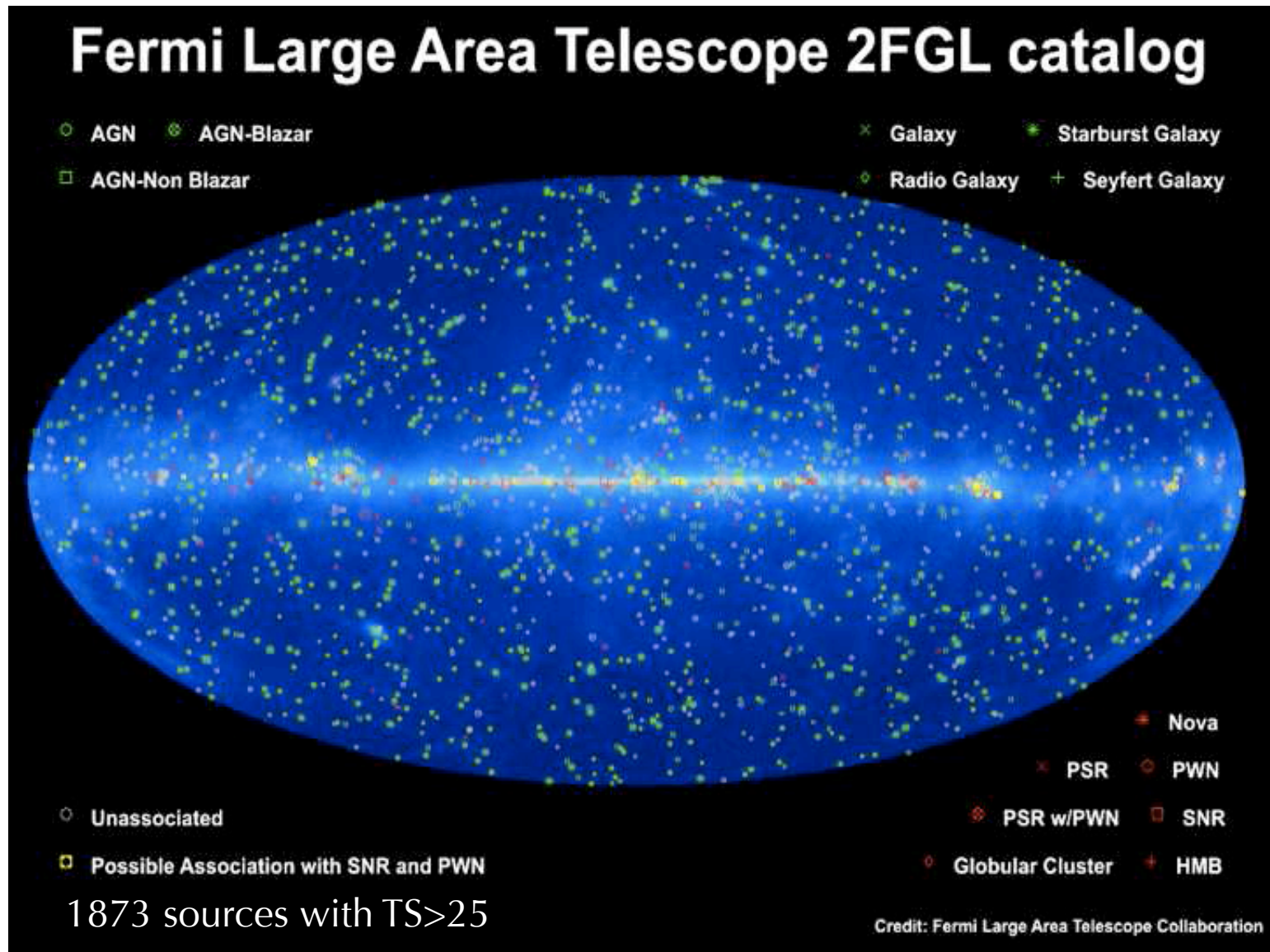
EGRET



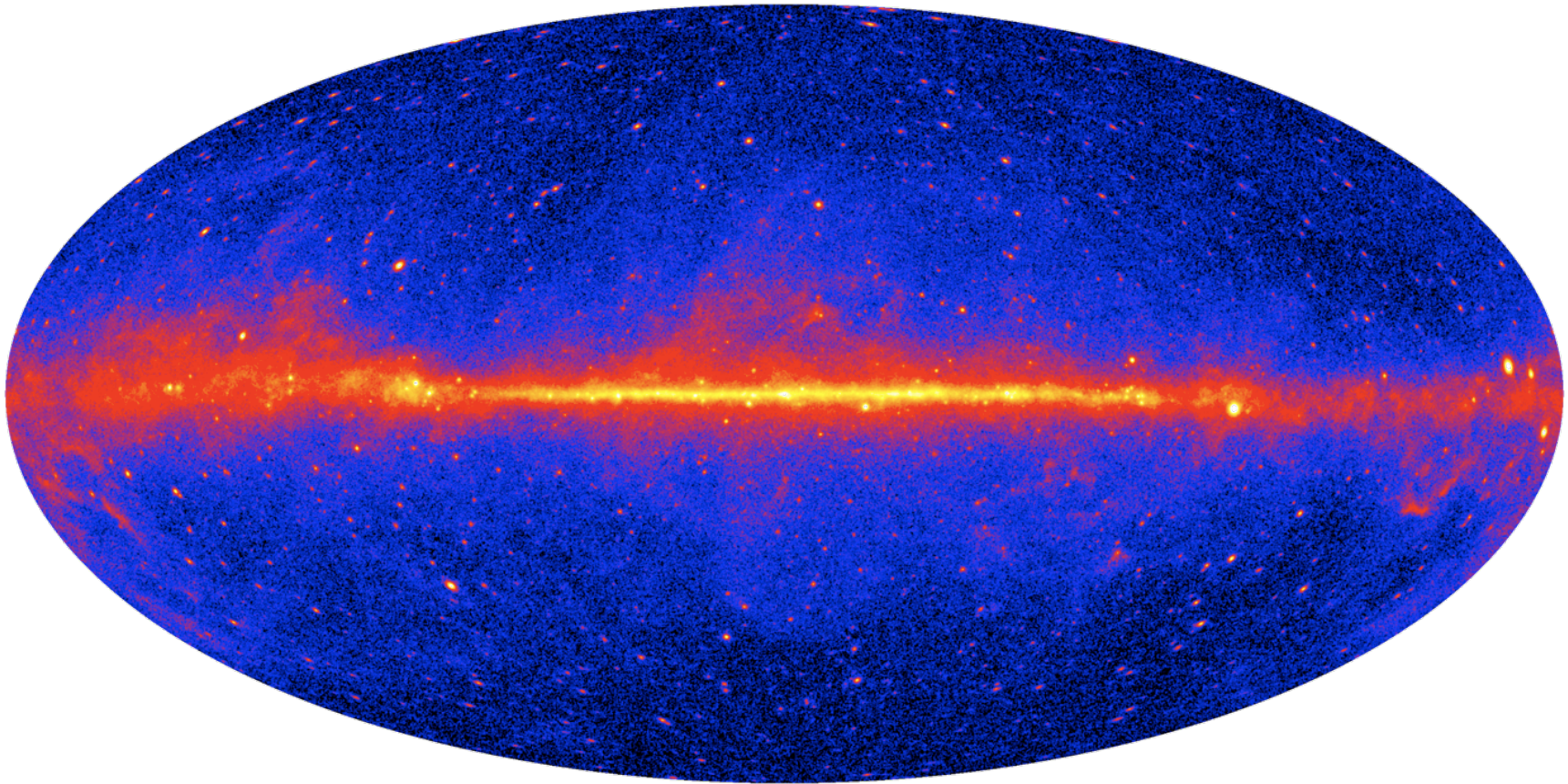
- $\sim 1.4$  M $\gamma$ ,  $\sim 60\%$  interstellar emission from the MW
- $\sim 10\%$  are cataloged (3EG) point sources

Slide from S. Digel

# Fermi-LAT 2FGL Skymap



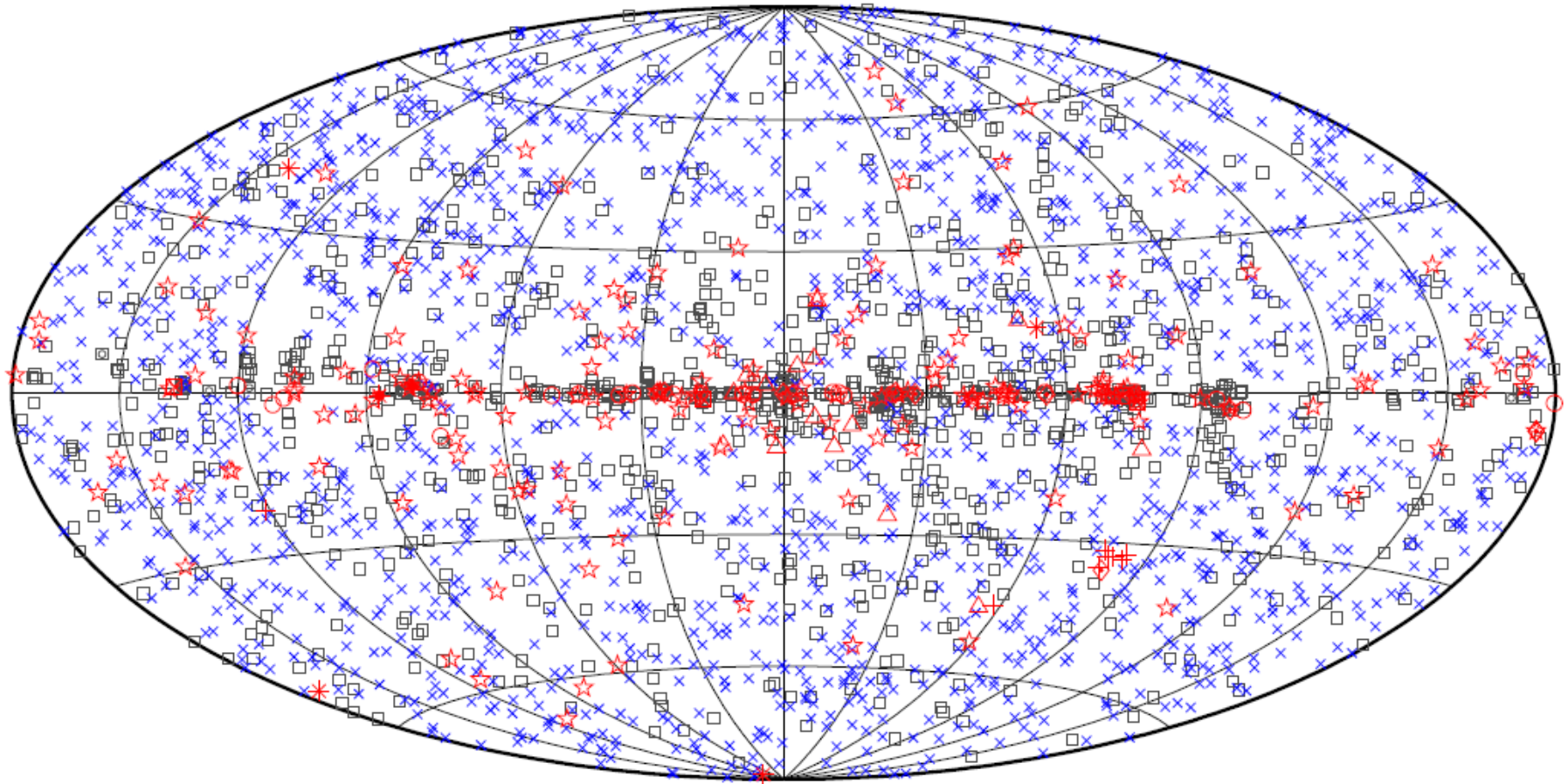
# Fermi-LAT 3FGL Skymap



- 4 years of data
- Energy range 100 MeV - 300 GeV
- 3032 sources, 2192 at  $|b| > 10^\circ$
- 3FGL Catalog Paper:



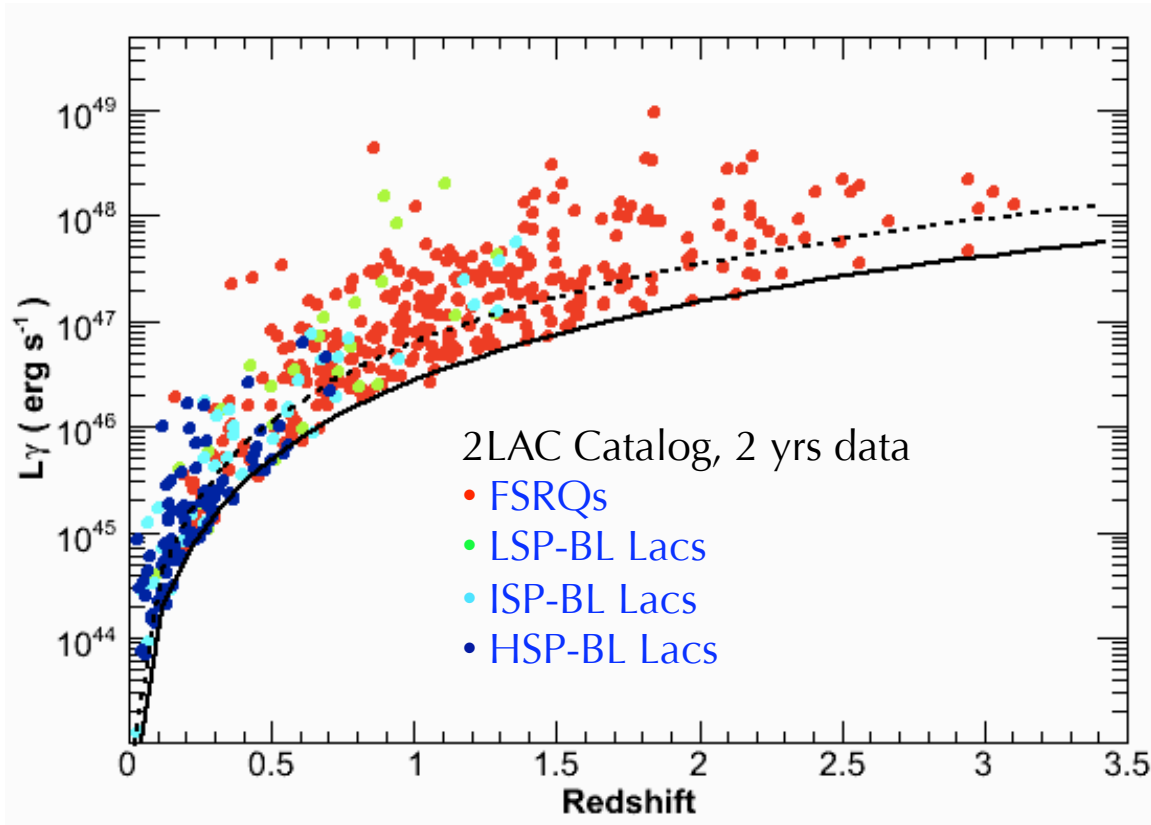
# Fermi-LAT 3FGL Point Sources



□ No association	◻ Possible association with SNR or PWN	× AGN
☆ Pulsar	△ Globular cluster	◇ PWN
⊠ Binary	+ Galaxy	⋆ Nova
★ Star-forming region	○ SNR	

3FGL AGN Catalog paper: <http://arxiv.org/pdf/1501.06054.pdf>

# GeV AGN



$$L_\gamma = 4\pi d_L^2 \frac{S(E_1, E_2)}{(1+z)^{2-\Gamma}}$$

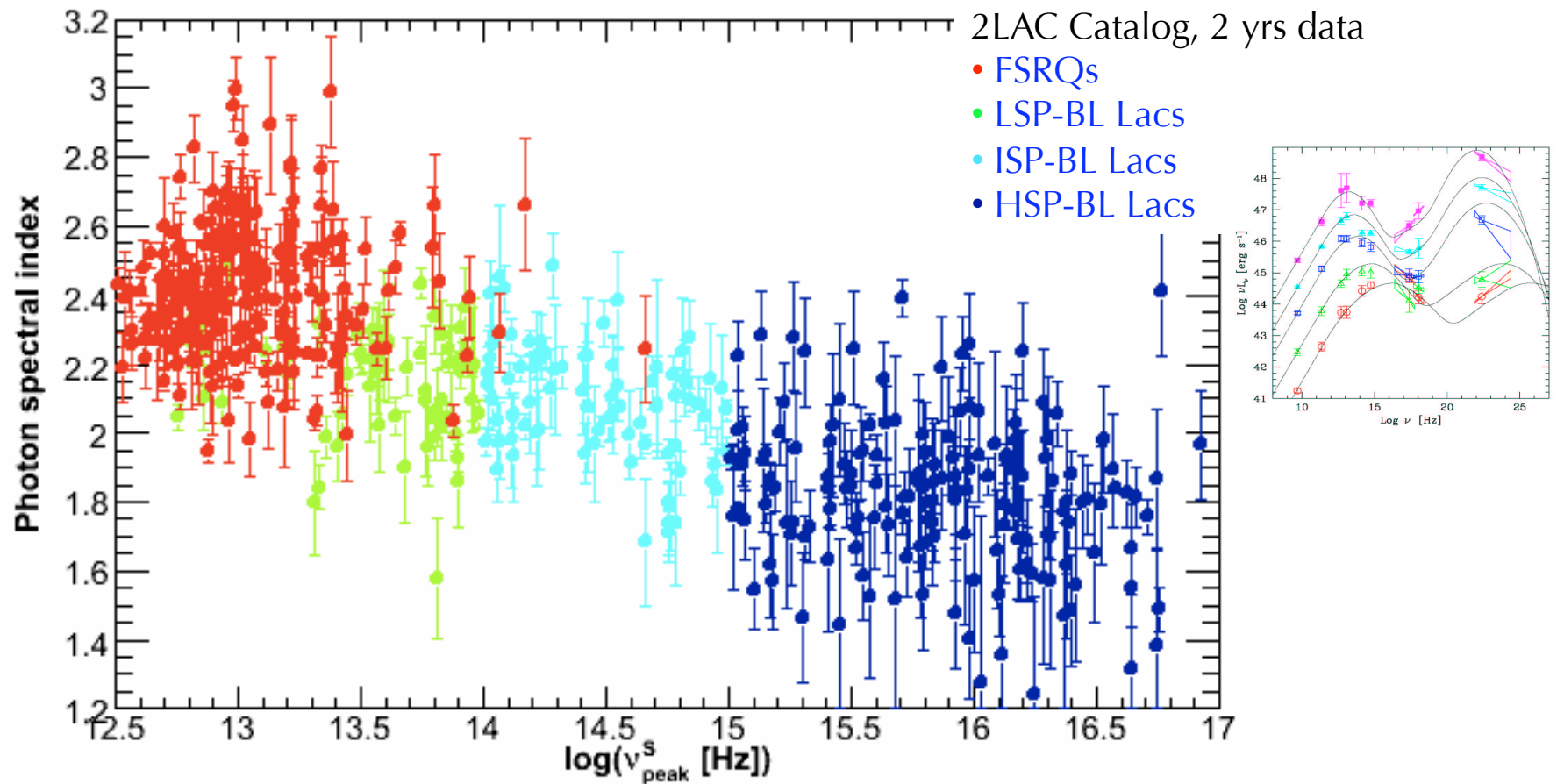
Only the most powerful FSRQs can be detected from large  $z$ :  
 $L_\gamma = 10^{46} (f_\gamma / 10^{-10} \text{ erg cm}^{-2} \text{ s}^{-1}) (d / 3 \text{ Gpc})^2 \text{ erg s}^{-1}$

$d_L$ : luminosity distance  
 $S(E_1, E_2)$ : energy flux between  $E_1$  (100 MeV) and  $E_2$  (100 GeV)

Note that these are apparent luminosities. We are seeing Doppler boosted radiation. Doppler factor  $\delta \sim 10$ -100.

3FGL AGN Catalog paper: <http://arxiv.org/pdf/1501.06054.pdf>

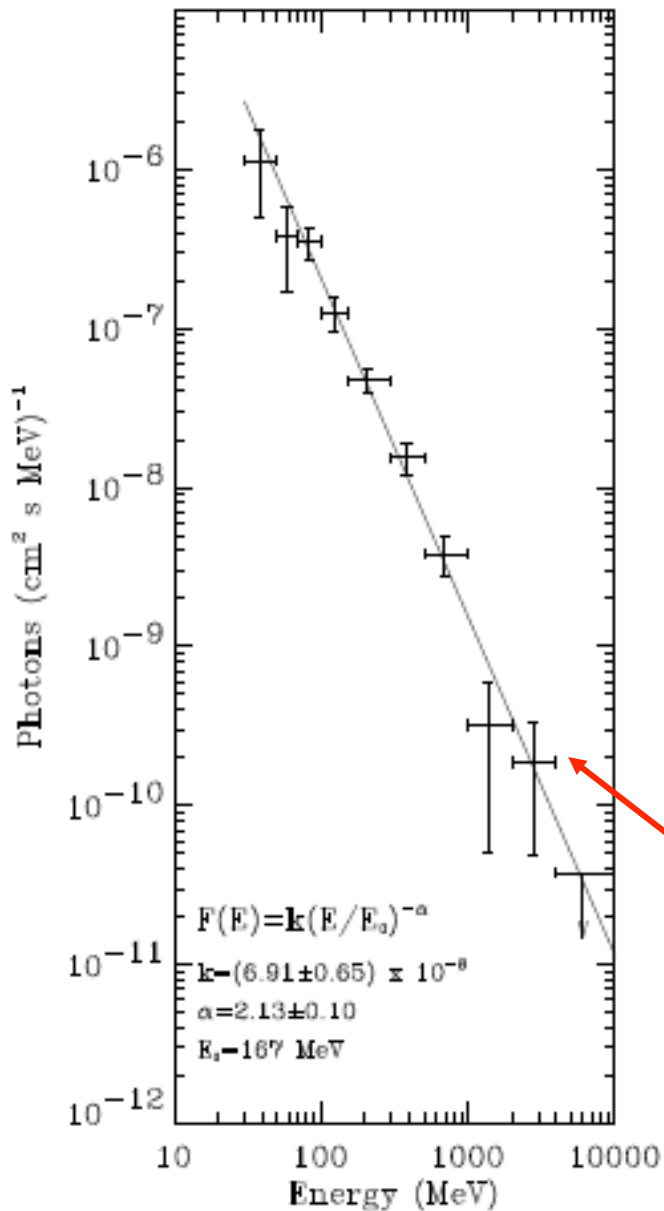
# Synchrotron Peak and Photon index



Correlation between photon spectral index measured with the LAT and position of the SED synchrotron peak

3FGL AGN Catalog paper: <http://arxiv.org/pdf/1501.06054.pdf>

0528+134 VP2130



## Blazars Detected above 100 MeV

- Power-law spectra in the energy range 30 MeV – 10 GeV.
- No evidence of spectral cutoff below 10 GeV

Steeply falling photon spectra – Poor statistics above  $\sim 10$  GeV.  
At very high energies blazar studies are carried out by ground-based ACTs – large collecting areas.

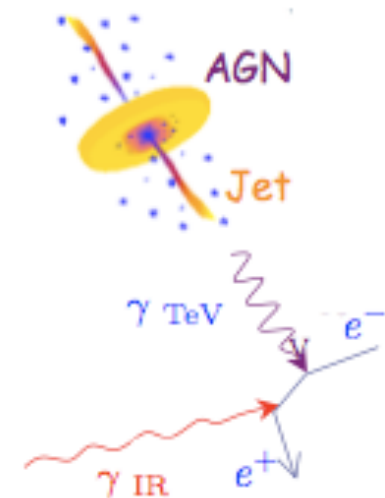
## VI. TeV Blazars

# Why study TeV blazars?



In addition to jet physics and properties of SMBHs and their environments....

- Particle acceleration and emission mechanisms?
  - General picture of jet structure & jet formation, acceleration & collimation?
  - Specific location of blazar outbursts?
  - TeV origin – particle content leptonic or hadronic?
  - Black hole – jet connection
- Best extragalactic probes of the EBL via its interaction with TeV photons traveling cosmological distances.
- Better constrain the IGMF.
- Test the validity of the Lorentz Invariance principle at high energies.
- Particle acceleration to extreme energies - origin of UHE cosmic rays ( $E > 10^{18}$  eV)?



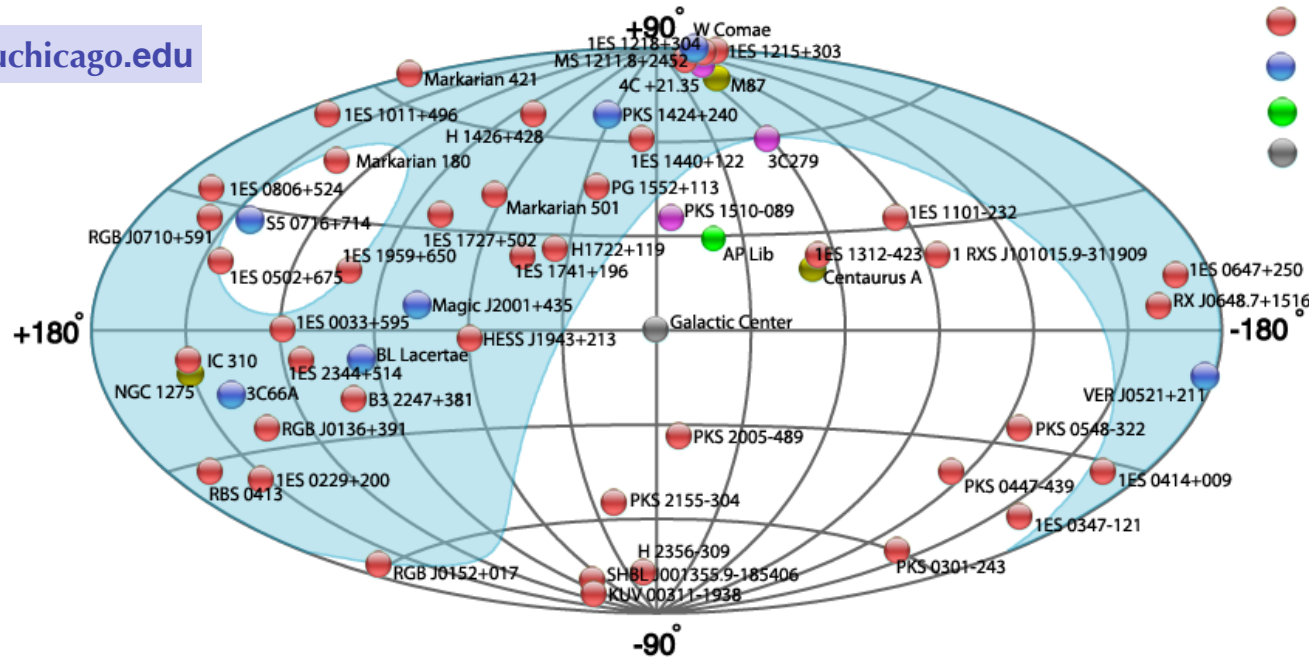
# The VHE Blazar Sky

## TeV Identified AGNs

### Source Types

- FSRQ
- FRI
- HBL
- IBL
- LBL
- UNID

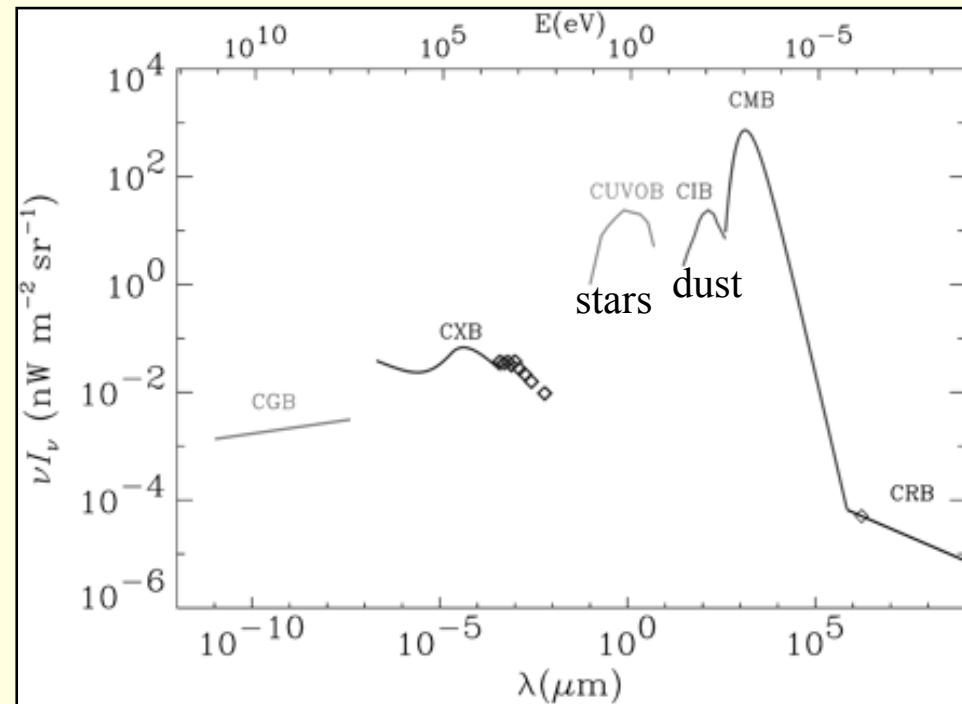
[tevcat.uchicago.edu](http://tevcat.uchicago.edu)



- Current generation of IACTs (H.E.S.S., MAGIC and VERITAS) has detected  $\gamma$ -ray emission from  $> 50$  AGNs. Redshift up to 0.944!
- Population is largely dominated by high-frequency peaked BL Lacs ( $\sim 80\%$ ), but also includes low-frequency peaked objects ( $\sim 20\%$ ), flat spectrum radio quasars, and radio galaxies.

# Extragalactic Background Light

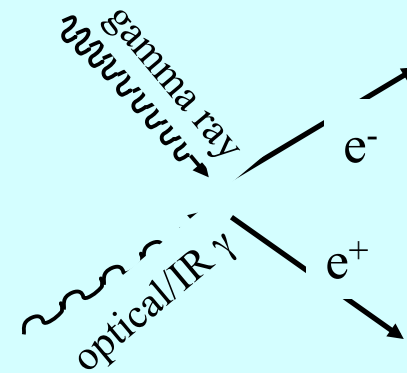
- Sensitive to star formation history
- Difficult to measure optical background directly



Hauser & Dwek 2001

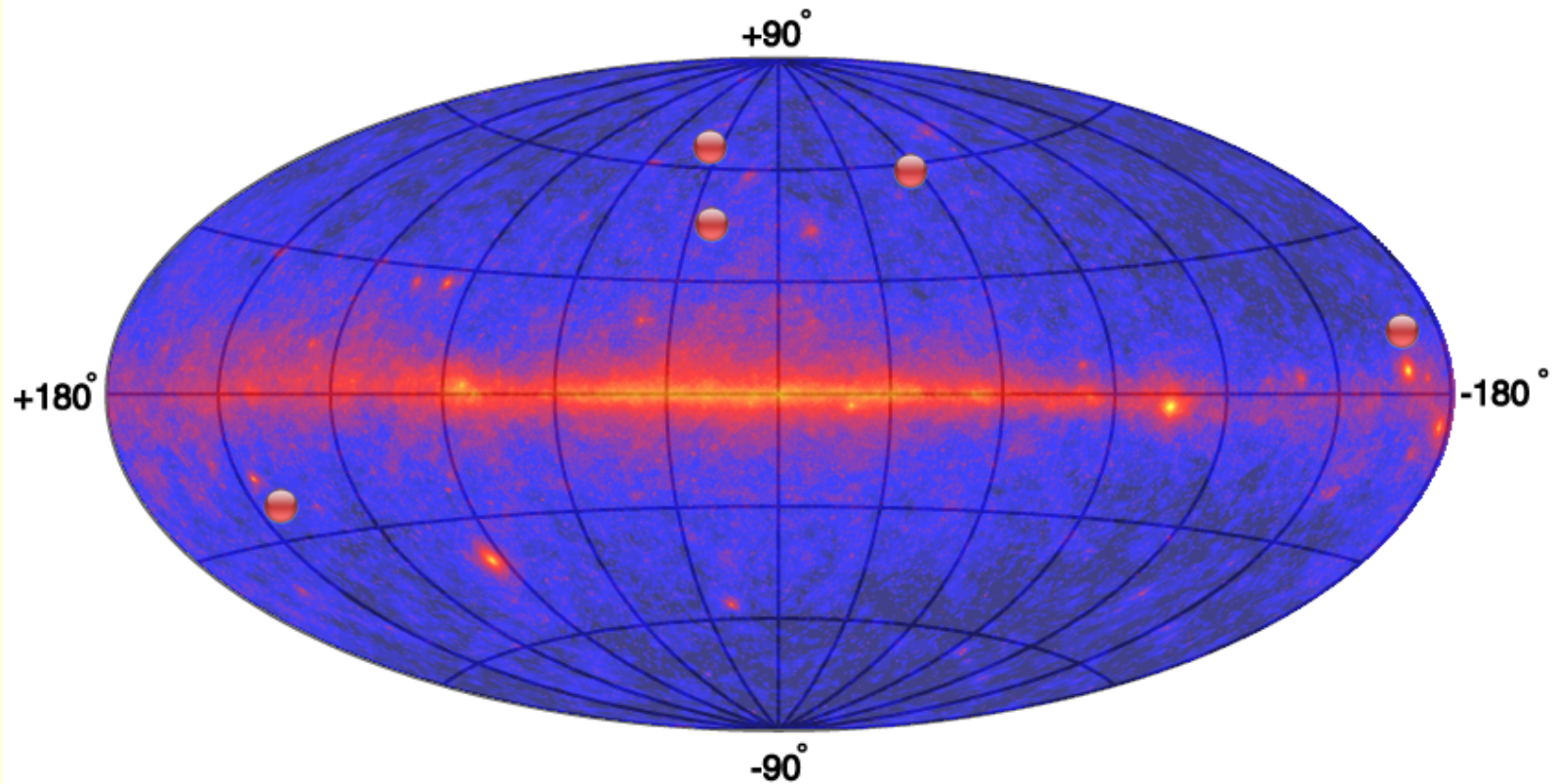
- $\gamma$ -rays pair produce with EBL photons
- Cross section:  $\lambda_{\text{peak}} = 1.33 \times (E/\text{TeV}) \text{ mm}$
- $> 100 \text{ GeV}$ , sensitive to UV/optical
- $> 1 \text{ TeV}$ , sensitive to IR EBL

## Gamma-ray absorption by EBL





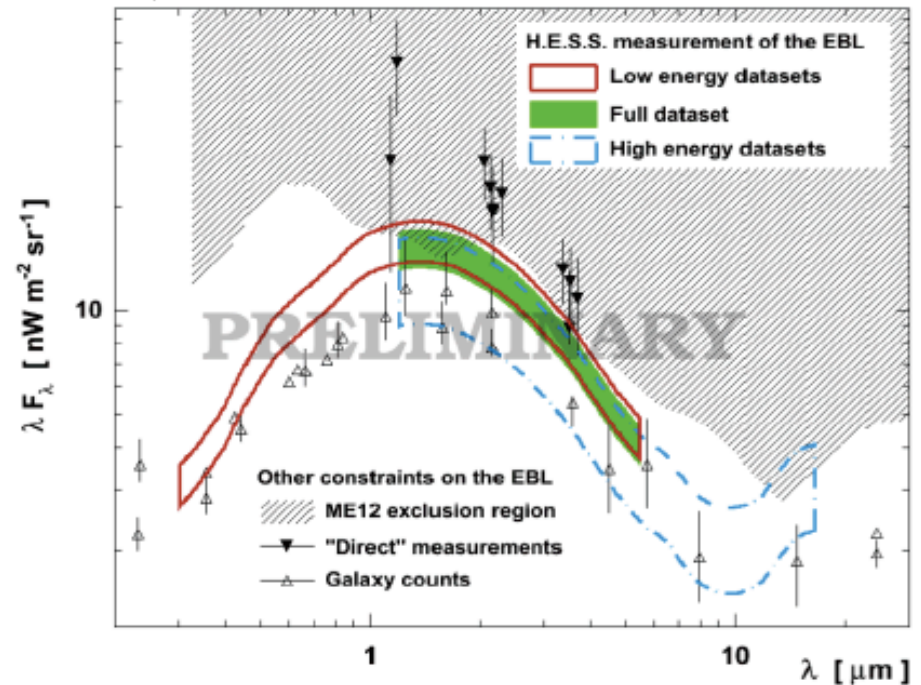
# High Redshift Blazars



S3 0218+35	02 21 05.5	+35 56 14	Blazar	2014.07	$z = 0.944$
PKS 1441+25	14 43 56.9	+25 01 44	FSRQ	2015.04	$z = 0.939$
3C 279	12 56 11.1	-05 47 22	FSRQ	2008.06	$z = 0.5362$
PG 1553+113	15 55 44.7	+11 11 41	HBL	2006.03	$z = 0.5$
1ES 0647+250	06 50 46.5	+25 03 00	HBL	2011.09	$z = 0.45$

# The EBL Imprint

- Allow for intrinsic source spectra with curvature
- Parametrization of the EBL optical depth via a scaling factor  $\alpha$
- Fit of a large VHE data set
  - 75 000  $\gamma$ -rays from the seven brightest blazars
  - Distance  $0.03 < z < 0.19$ ,
  - 400 hours of observation with H.E.S.S.



See Talk by Christian Stegmann | H.E.S.S.  
Highlights | Gamma 2012

# High-redshift Source

Oldest VHE  $\gamma$ -rays in Universe from a source at red shift of  $z = 0.944$  detected

**Discovery of Very High Energy Gamma-Ray Emission From Gravitationally Lensed Blazar S3 0218+357 With the MAGIC Telescopes**

ATel #6349; *Razmik Mirzoyan (Max-Planck-Institute for Physics) On Behalf of the MAGIC Collaboration*  
on 28 Jul 2014; 14:20 UT  
Credential Certification: *Razmik Mirzoyan (Razmik.Mirzoyan@mpp.mpg.de)*

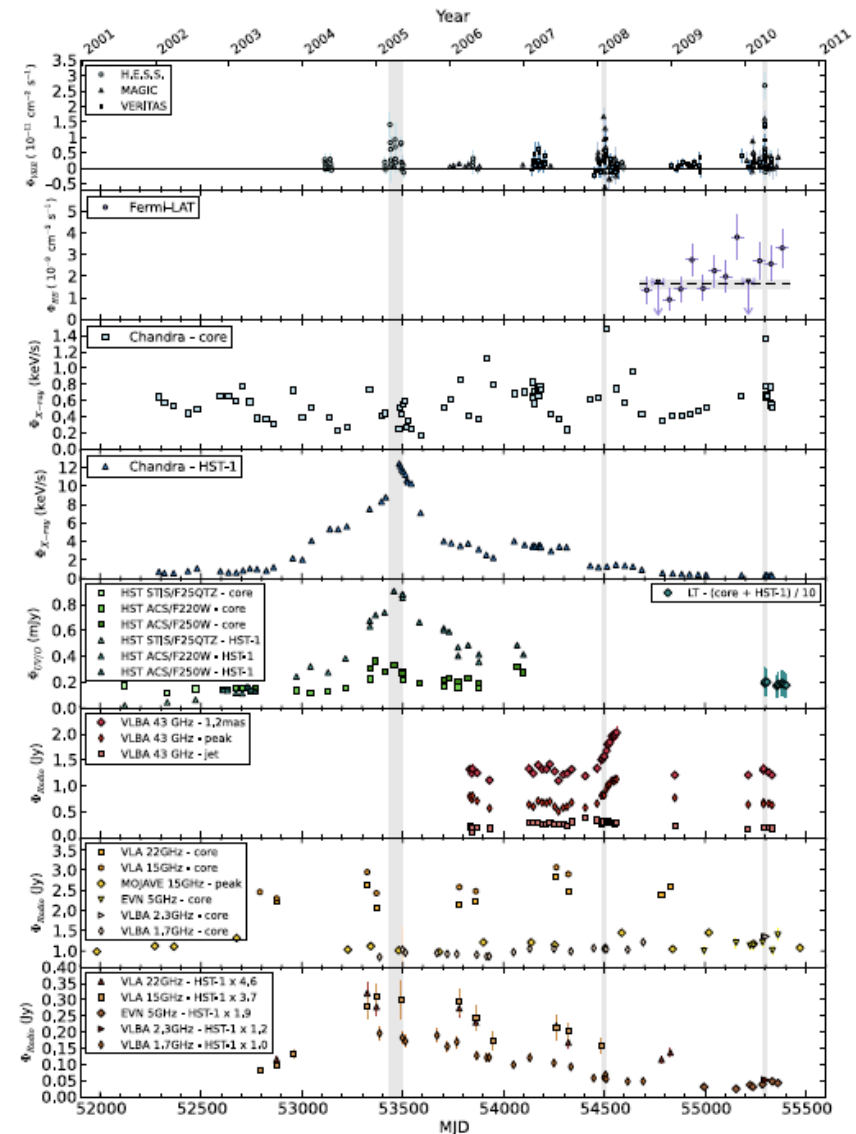
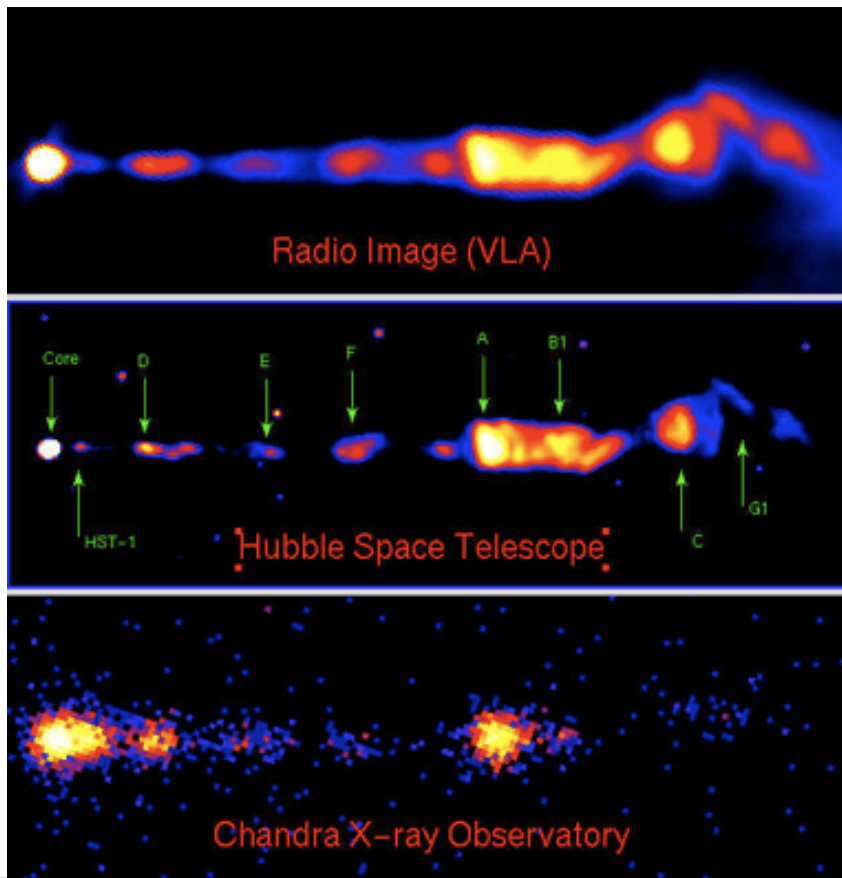
- On a few occasions Fermi mission measured flares of the blazar S3 0218+357 *with a time lag of 11.5 days.*
- This was interpreted as due to the gravitational lensing effect
- 2 weeks ago MAGIC detected a flare with  $> 5 \sigma$  at the anticipated time of the arrival of Fermi gravitational lense echo
- The most distant source discovered @ VHE !

See Talk by

Razmik Mirzoyan: VHE Gamma-Astrophysics with IACTs:  
1989-2014, 3rd October 2014, "LHC Days in Split", Split, Croatia

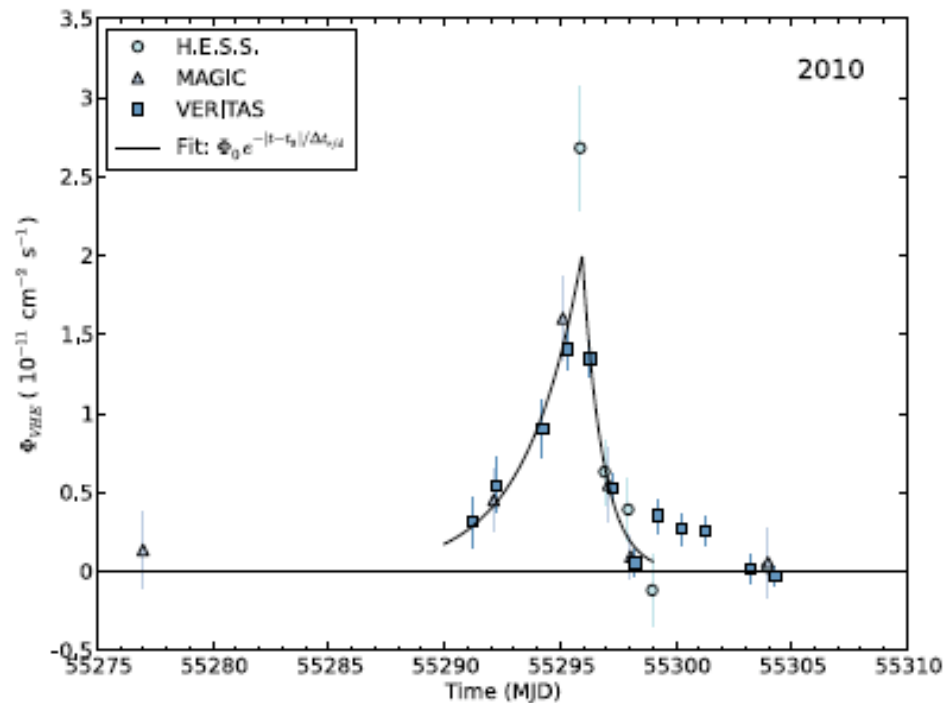
# Radio Galaxies: M 87 - A very close AGN

- Location of the emission region ----
- M 87 is one of the closest AGNs (20 Mpc).  
The jet is oriented at  $\sim 20^\circ$
- VHE studies are likely to contribute to a better understanding of AGN unification schemes

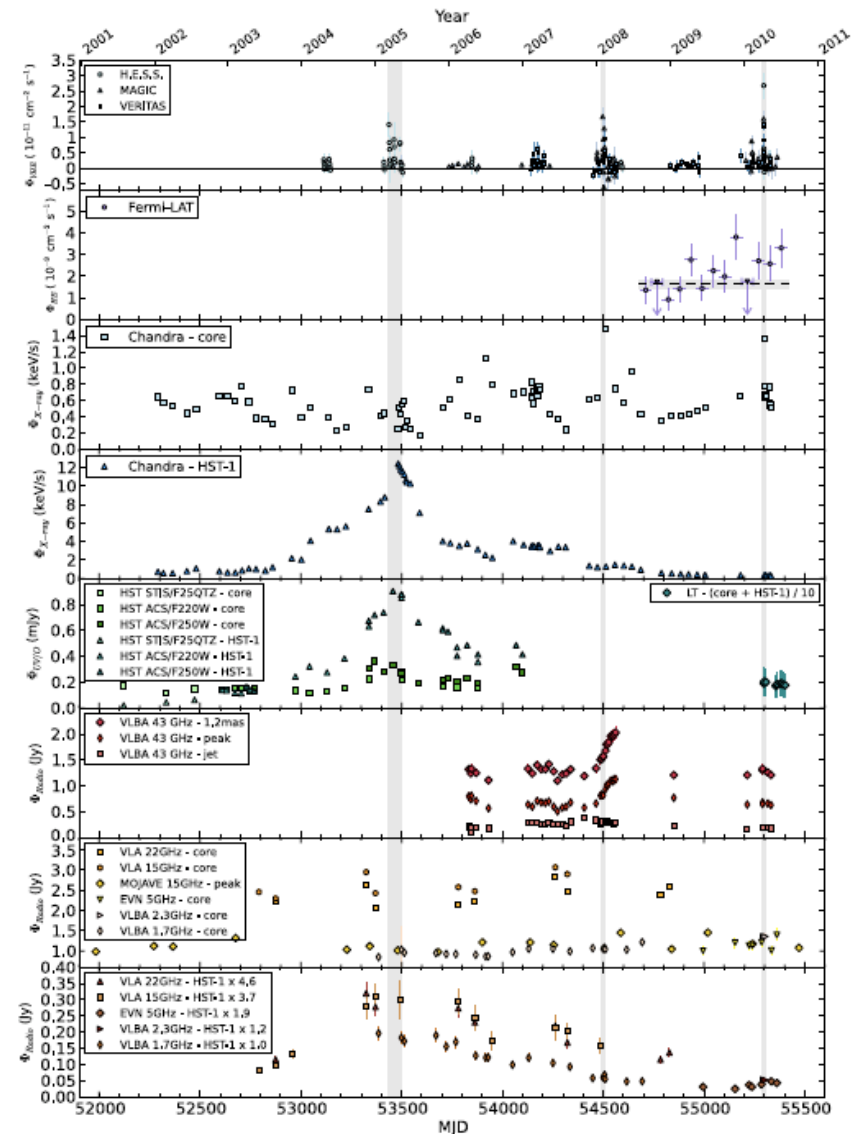


Abramowski et al. 2012

# Radio Galaxies - M 87 - A very close AGN



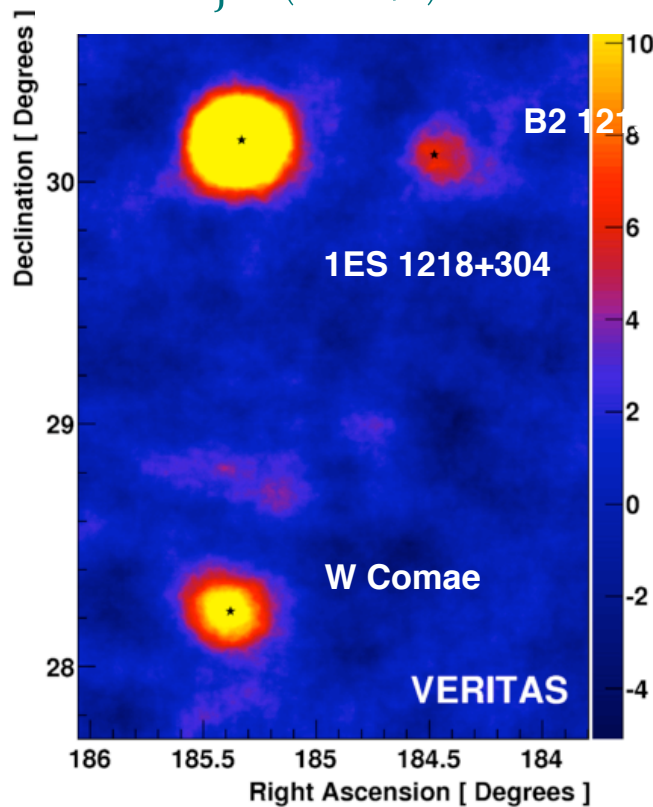
- VHE light curve of M 87 zoomed on the 2010 flare.
- VHE temporal behavior characterized –
- $\tau_{\text{rise}} = \sim 1.7$  days and  $\tau_{\text{decay}} = \sim 0.61$  days



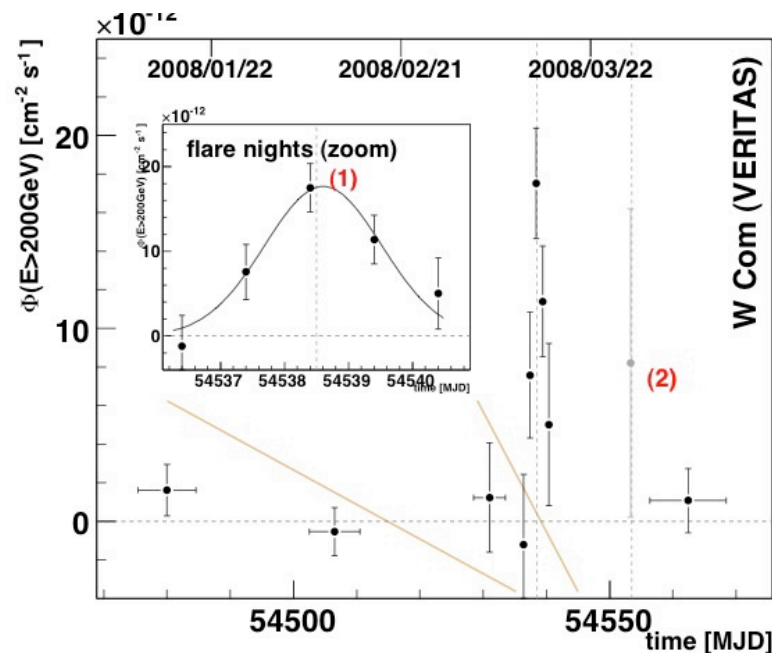
Abramowski et al. 2012

# VERITAS: Typical Blazar Luminosities

- Blazars detected as point sources at TeV
- Variable sources; variability could be  $\sim$  day-scale or sub-hour
- VHE  $\gamma$  rays during W Comae flare  $\sim 25\%$  of the flux of the Crab Nebula ( $> 200$  GeV). Luminosity  $\sim 10^{45}$  ergs/s. Only a very small fraction of the blazar jet ( $< 10\%$ ) accounts for this luminosity.



Benbow et al. ICRC 2011

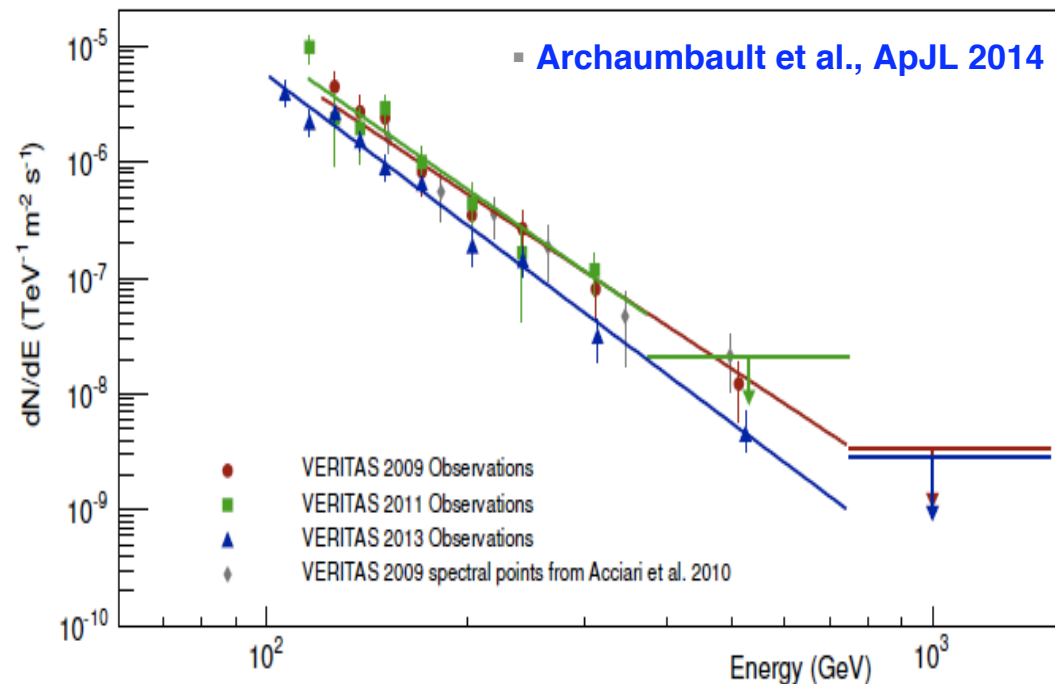


Acciari et al. 2008 ApJ 690, L73

- 70% of excess from 4-night flare in 2008 March
- $275\gamma$ ,  $8.6\sigma$ ;  $\tau \approx 1.3 \pm 0.3$  days, 9% CU

# Deep Broadband Observations of the Distant $\gamma$ -ray Blazar PKS 1424+240

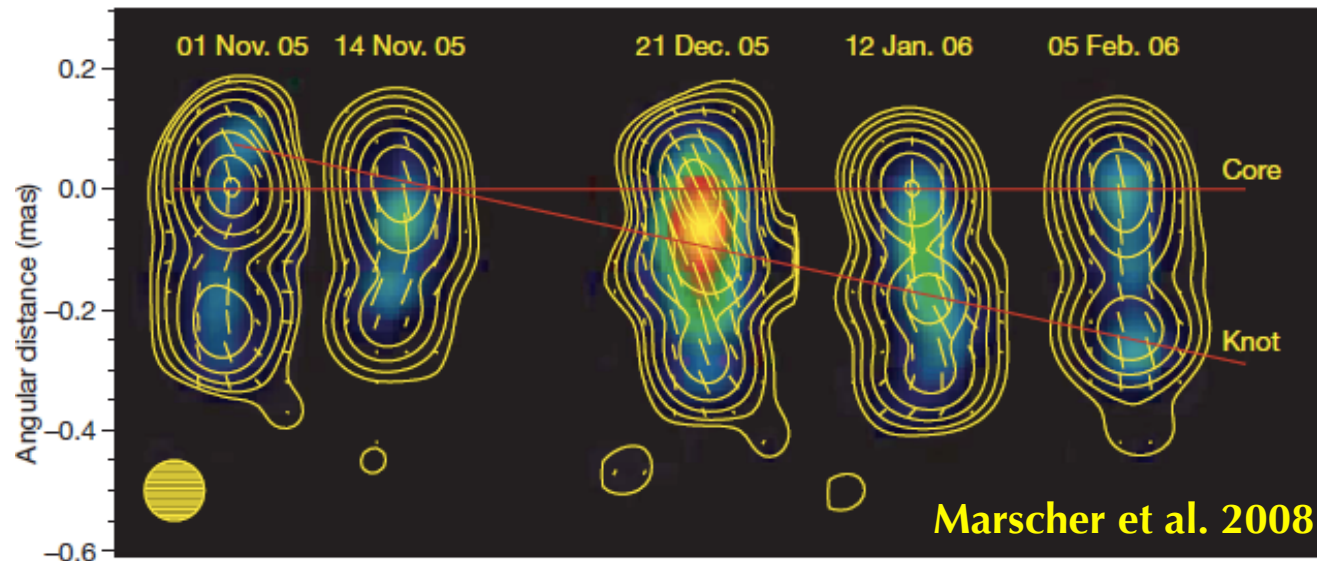
- Detected at VHE by VERITAS in 2010. Deep campaign: >100 hours of new data since 2010
- HST/COS obs. :  
 $z > 0.6035$  (Furniss et al., 2013)
- *At this minimum distance, the intrinsic VHE emission is expected to be significantly absorbed by the extragalactic background light (EBL)*



- Observed VHE spectra of PKS1424+240 derived from three years of VERITAS observations show no significant evidence of spectral variability

# Locating the Emission Region in the Jet

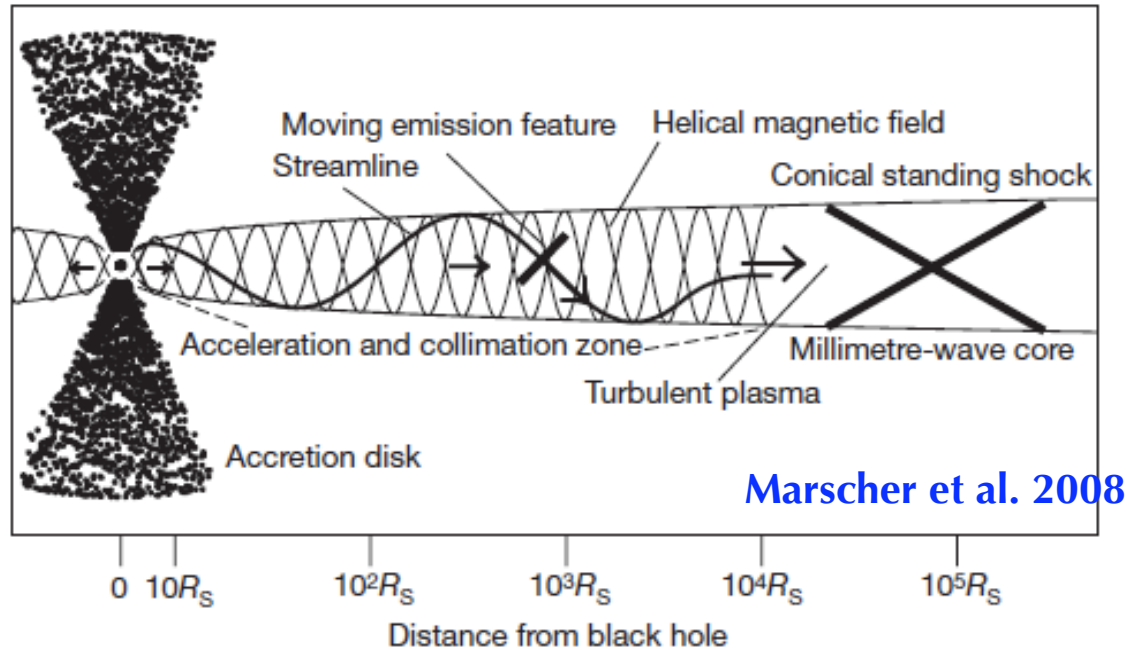
The jet of BL Lac - Sequence of VLBA images at a  $\lambda$  of 7mm (43 GHz).



- Blazar at a redshift of 0.069 (291 Mpc)
- VHE emission detected by MAGIC in 2005
- Angle of BL Lac jet to our line of sight: 6–10°. Flow speed: of 0.981–0.994c. Corresponding Lorentz factor:  $\sim 7$  (Jorstad et al. 2005)
- Relativistic aberration and the Doppler effect strongly beam the radiation, high apparent luminosity.
- Knot's observed proper motion of 1.2 mas/yr ( $\sim 5.0c$ ) (Marscher et al. 2008)

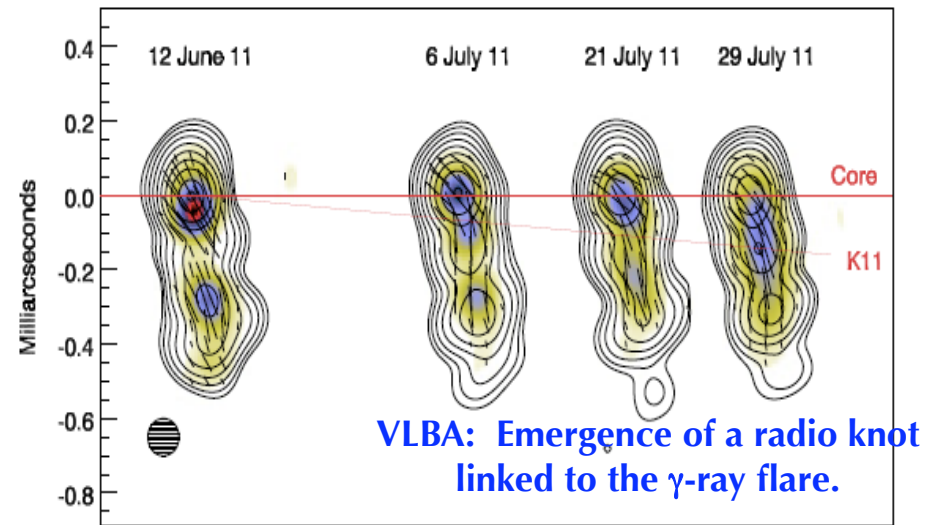
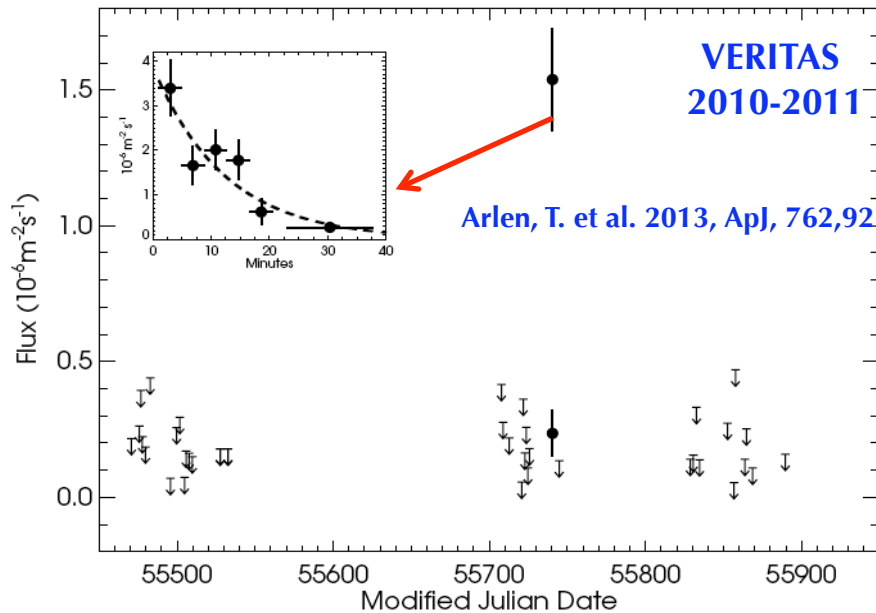


# A Proposed Model of the Inner Jet



- Where is the energy dissipated in the jet? What fraction of the jet is responsible for the observed luminosity?
- Data from radio + TeV  $\gamma$ -ray flare seem to indicate that the core is a standing shock located well downstream of the BH.
- Radiating plasma follows a helical magnetic field configuration upstream of the radio core (Marscher et al. 2008).
- Radio observations probe outer regions of the jet (pc scale). [TeV  \$\gamma\$ -ray observations](#) powerful tool for probing inner regions of jets.

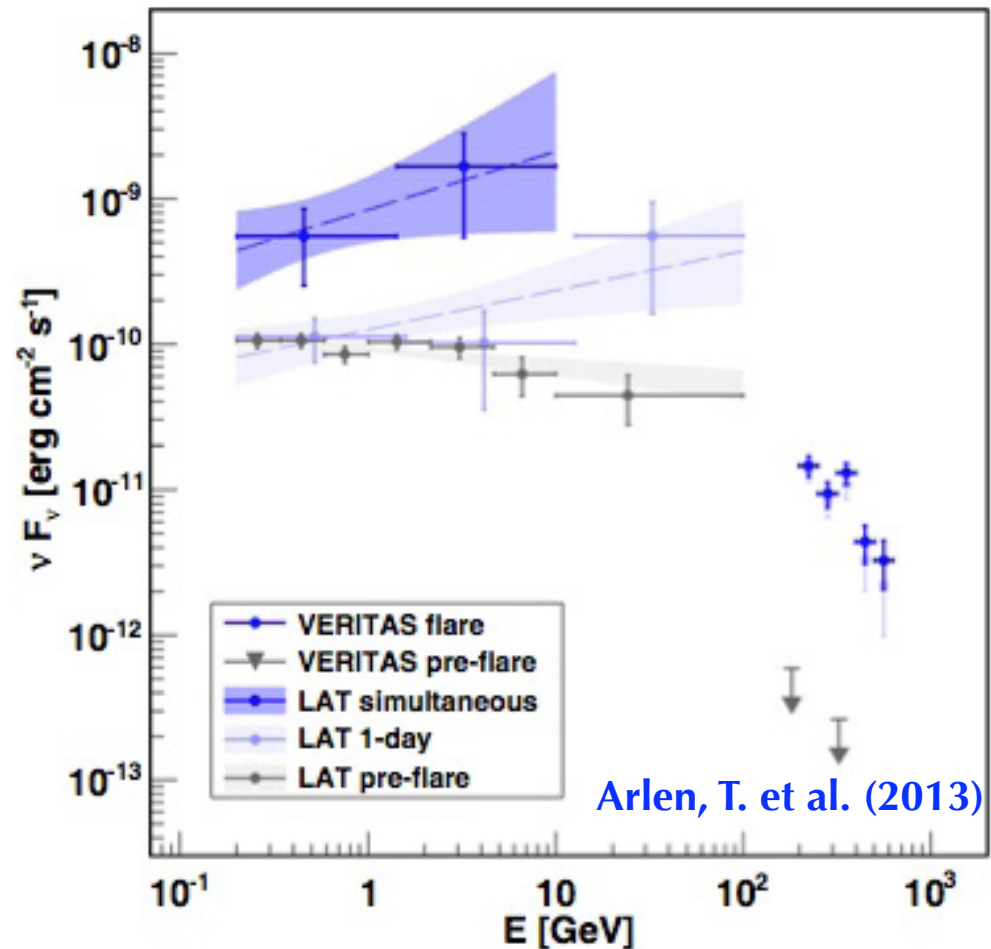
# BL Lac: TeV Flare and Rapid Variability



- Flare on June 28, 2011 picked up by VERITAS monitoring; 4-min bins; 125% Crab flux ( $> 200$  GeV);  $\Gamma = 3.8 \pm 0.3$ ; good MWL coverage.
- Flux decayed by factor of 10 in  $\tau = 13 \pm 4$  min  $\Rightarrow$  Strongly constrains size of emission region ( $R < c\tau\delta/(1+z) \sim 2.2 \times 10^{13} \delta$  cm) (independent of any model).
- Flares + MWL coverage provide remarkable tomography of jet.
- New SL component near core (43 GHz) - new knot K11, shows a different polarization position angle ( $20^\circ$  compared with  $44^\circ$  for the core).

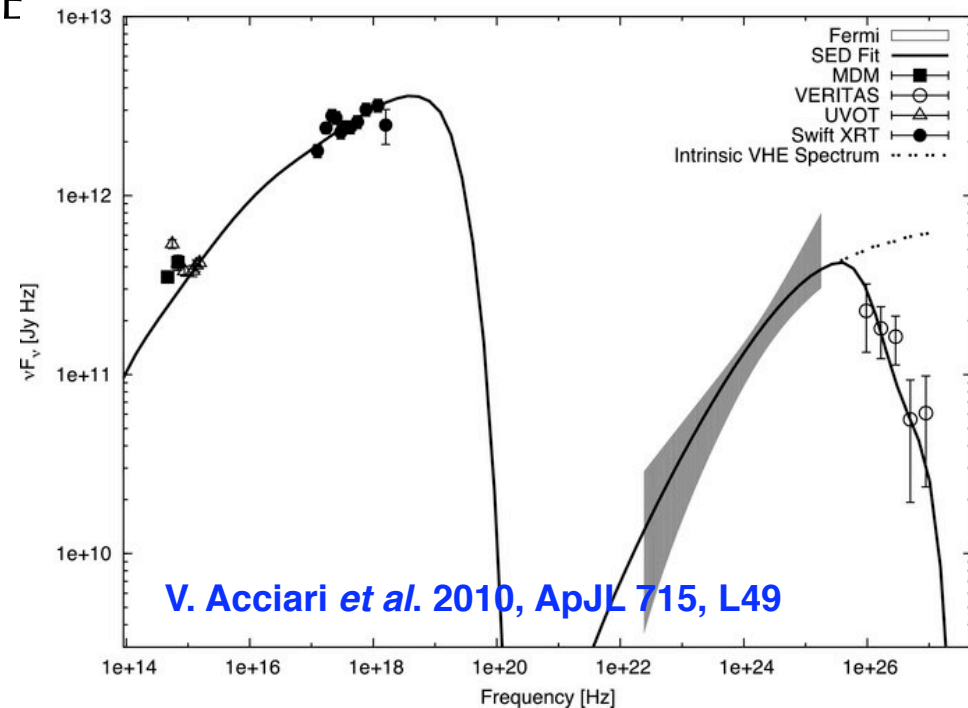
# BL Lacertae flare & pre-flare SED

- TeV flare occurred when source was active & variable in GeV band.  $\gamma$ -ray SED peak lies  $\sim 10$ - $100$  GeV.
- LAT data shows evidence for spectral hardening during the VERITAS flare.
- Sharp break at TeV energies – Klein-Nishina effects  
( $h\nu_0 \geq mc^2/4\gamma_{KN}$  - electron cooling rate is substantially reduced)



# HBLs: RGB J0710+591

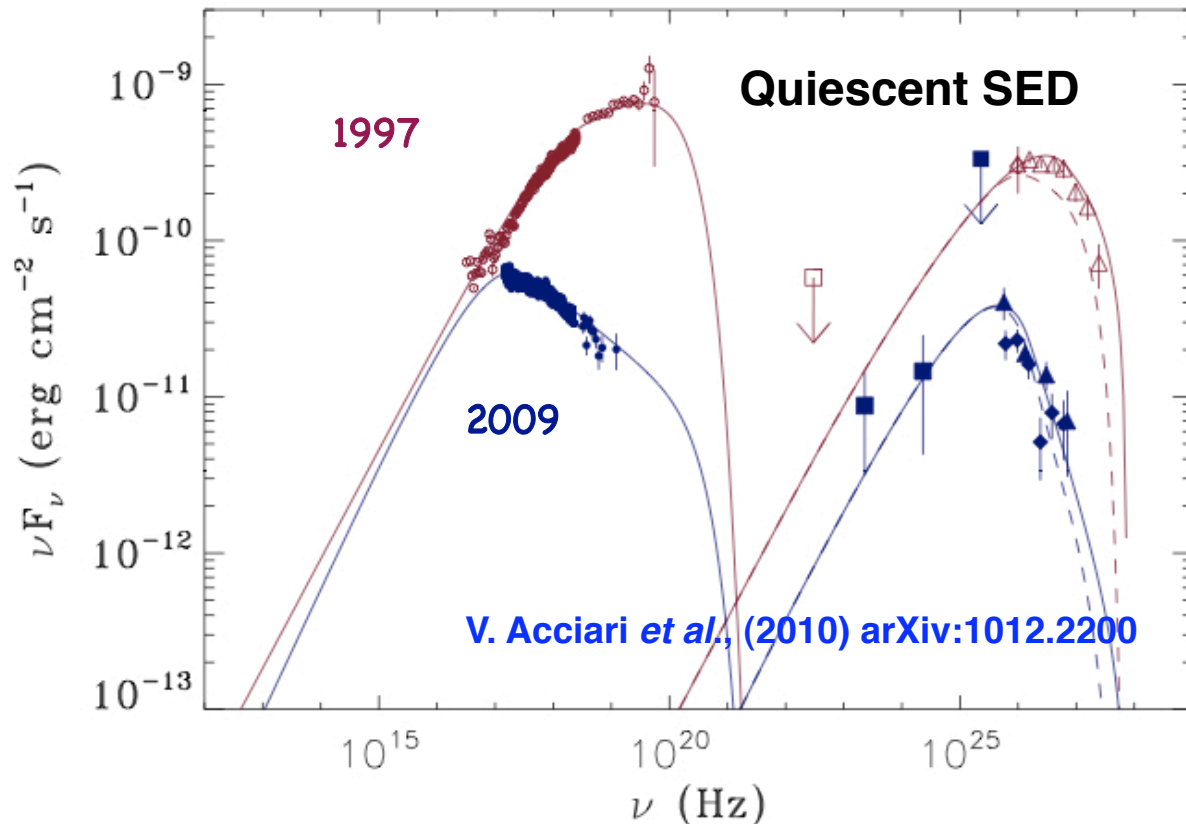
- “Extreme” HBL. Promising VHE candidate
- Redshift 0.125
- Useful for EBL studies
- VERITAS detection triggered observations at other wavelengths, including Fermi-LAT detection
- First Fermi-LAT source found with VHE guidance



$$\Gamma_{\text{HE}} = 1.46 \pm 0.17_{\text{stat}} \pm 0.05_{\text{sys}}$$
$$\Gamma_{\text{VHE}} = 2.69 \pm 0.26_{\text{stat}} \pm 0.20_{\text{sys}}$$

## **Characterizing the Brightest Blazars....**

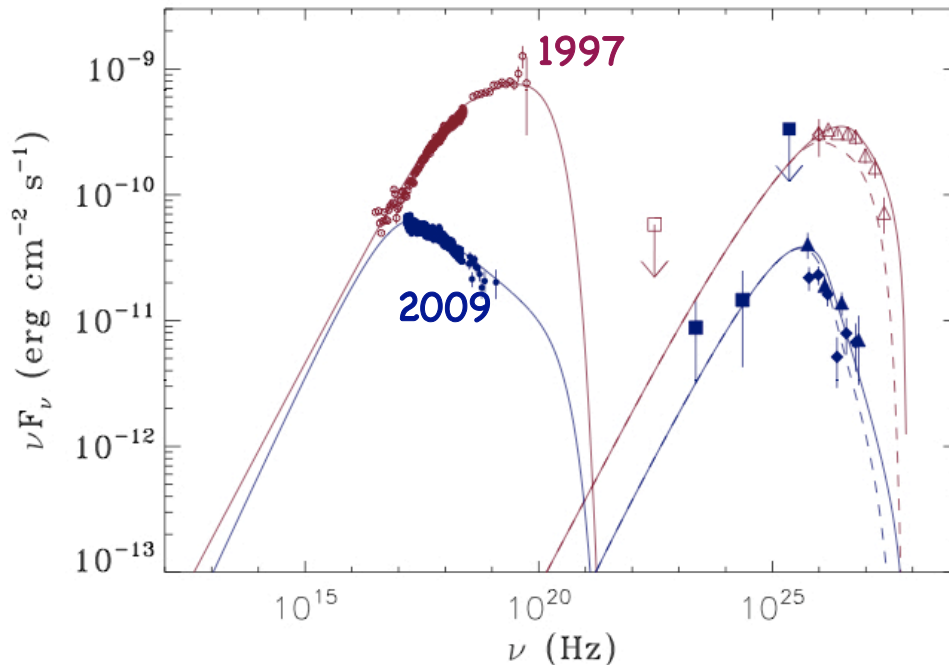
# TeV Blazars: Mrk 501



- Joint MWL campaign with MAGIC, Fermi-LAT, Suzaku. Data provides high quality sampling of quiescent broadband SED of Mrk 501
- Large shift in synchrotron peak; little shift in IC peak
- Both epochs well described by SSC model
- IC peak position primarily from onset of K-N suppression

# TeV Blazars: Mrk 501

V. Acciari *et al.*, (2010) arXiv:1012.2200

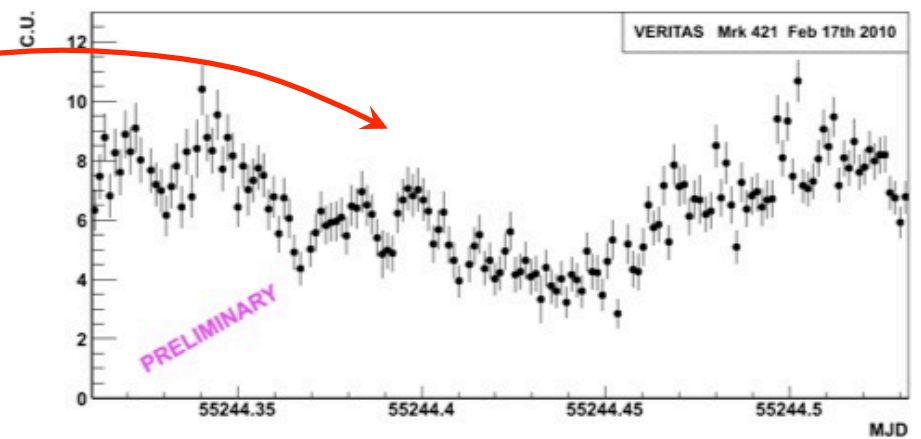
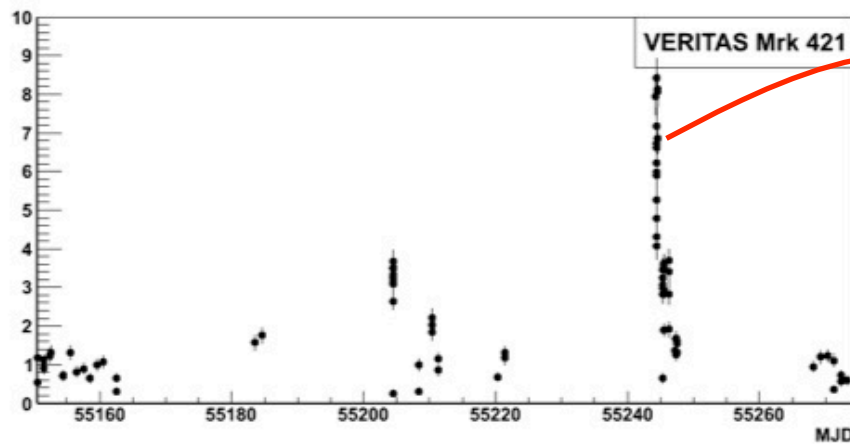
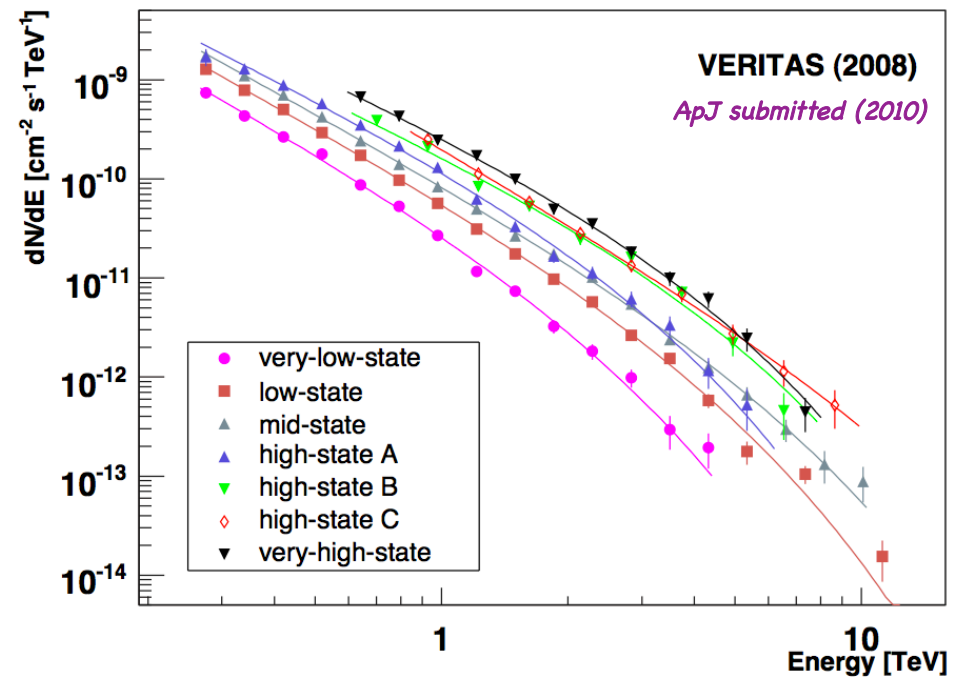


- X-ray data used to place limits on peak frequencies:
  - 230 keV ( $5.5 \times 10^{19}$  Hz) – high
  - 0.6 keV ( $0.6 \times 10^{17}$  Hz) – low
- Shift in VHE peak not as dramatic
  - Could be from onset of KN suppression
  - KN effects become important above  $h\nu \sim m_e c^2$  in electron rest frame

- $\gamma_e$  is characteristic Lorentz factor of  $e^-$  contributing to bulk of Xray emission.  
 $E_{\text{peak}}$  is peak energy on synch model
- Using  $D=20$ ,  $E_{\text{peak}} \sim 7.4$  keV for 1997 &  $\sim 46$  eV for 2009
  - For 1997,  $\gamma h\nu_{\text{peak}} \sim 1.1 \times 10^4$  MeV (extreme KN)
  - For 2009,  $\gamma h\nu_{\text{peak}} \sim 4.6$  MeV (moderately above KN)

# TeV Blazar: Mrk 421

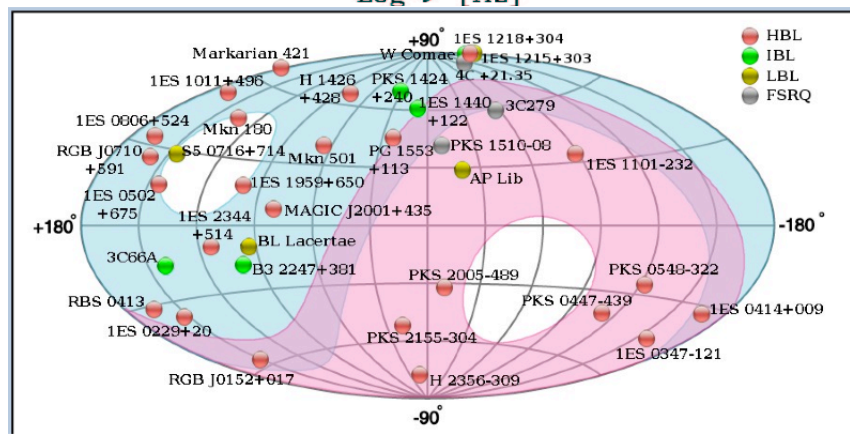
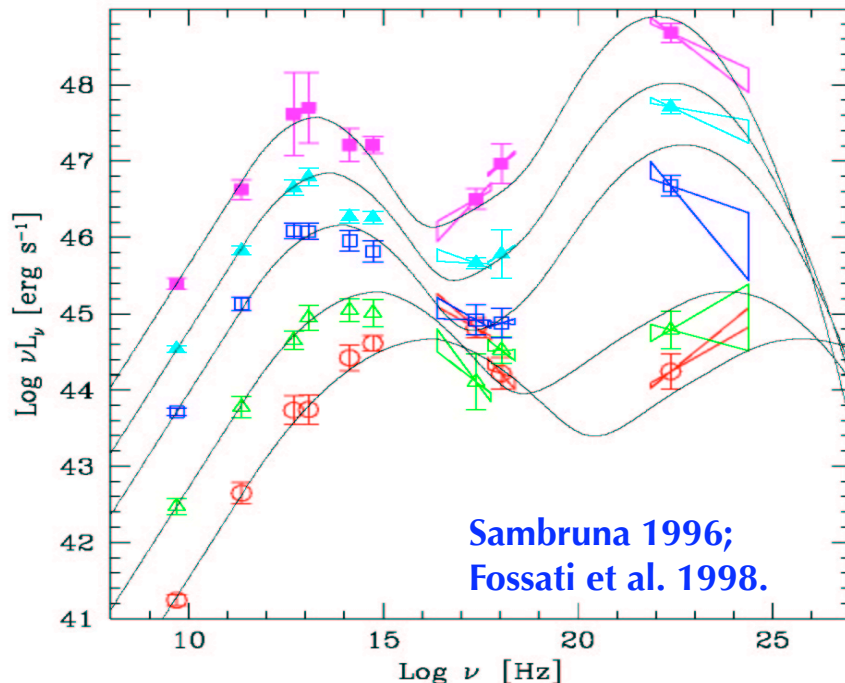
- long-term monitoring program
- major flares in 2008 & 2010
  - initiated large MWL efforts
  - spectral hardening with increasing flux
- high in VHE & X-ray since 11/09
  - 35 h of data;  $\sim 400\sigma$
- huge flare on Feb 17th 2010
  - variability on 5-10 min time scales
  - $>10\sigma$  per 2 minute bin





## VII. GeV-TeV Blazar Populations

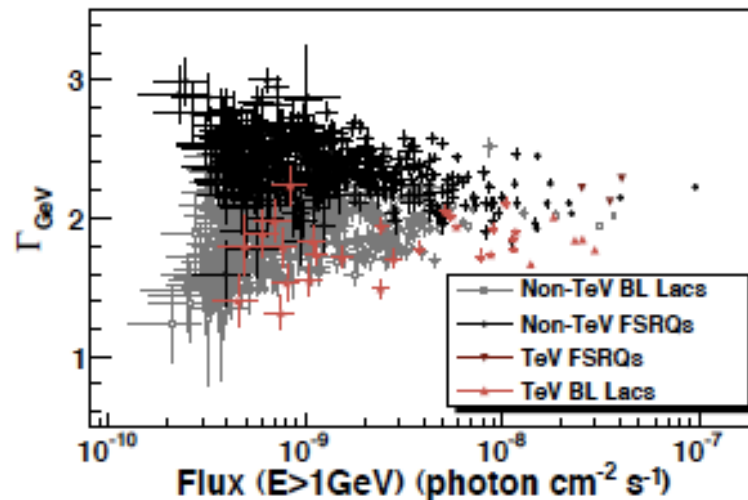
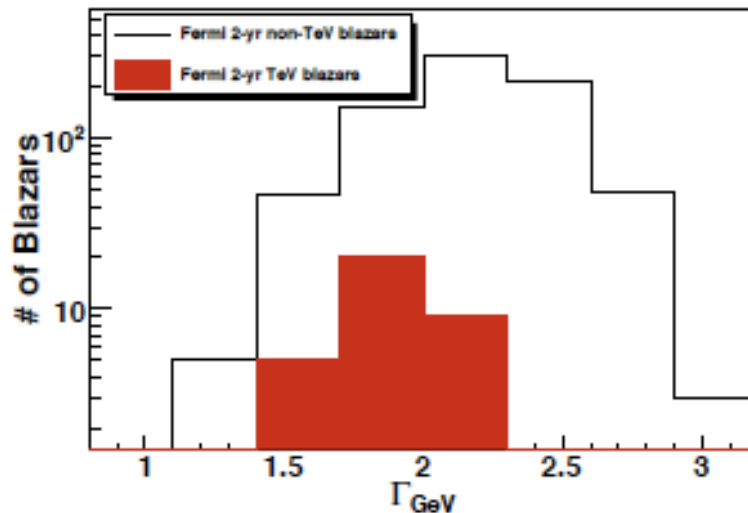
# Blazar SEDs



- The lack of sufficient number of GeV-TeV blazars limits our understanding of the  $\gamma$ -ray emission, and our ability to extrapolate results to the larger population of radio sources
- Fermi data for  $> 2$  yr available, now good coverage at  $\sim 100$  GeV.
- Underrepresented TeV blazar classes detected (IBLs, LBLs, FSRQs) --> start population studies.
- TeV blazars are now over 50 in number and with Fermi we get a good spectral coverage over 5 decades in energy that allows to start treating TeV as a population.

# GeV-TeV Blazars

Senturk et al. 2013



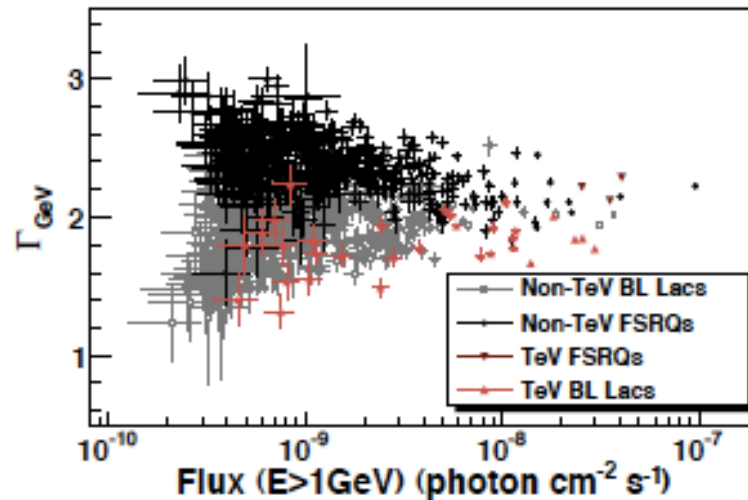
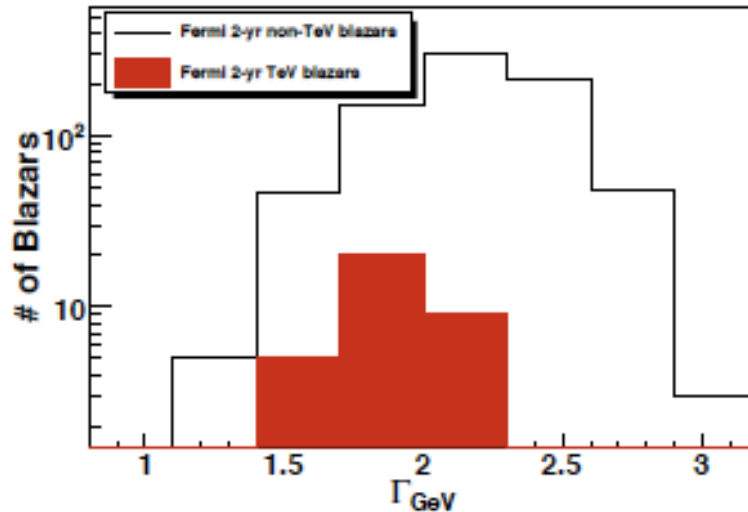
- Only a small fraction of Fermi blazars are TeV emitters.

- Top: distribution of Fermi spectral indices ( $\Gamma_{\text{GeV}}$ ) for TeV and non-TeV blazars in the 2FGL catalog. TeV -detected blazars tend to have harder GeV indices.

- Bottom:  $\Gamma_{\text{GeV}}$  vs. integral flux for  $E > 1 \text{ GeV}$ . For all TeV blazars,  $\Gamma_{\text{GeV}} < 2.3$  and for most of them  $\Gamma_{\text{GeV}} < 2$ , in agreement with an inverse-Compton peak frequency (IC) located in the high-energy tail of the Fermi range or beyond.

# GeV-TeV Blazars

Senturk et al. 2013



- Only a small fraction of Fermi blazars are TeV emitters.

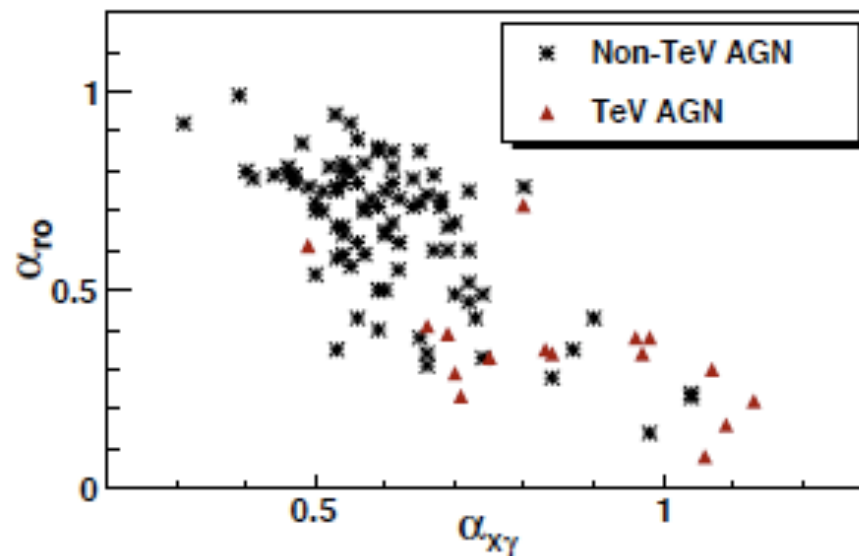
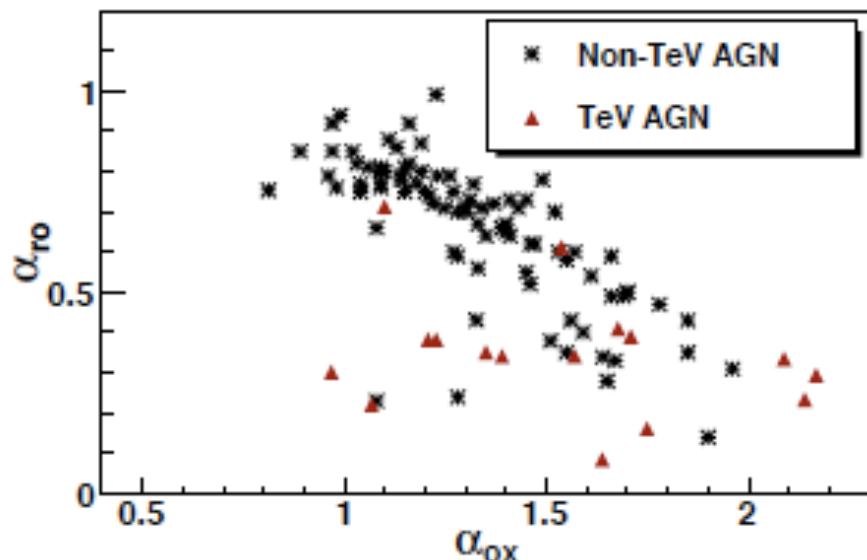
- Top: distribution of Fermi spectral indices ( $\Gamma_{\text{GeV}}$ ) for TeV and non-TeV blazars in the 2FGL catalog. TeV -detected blazars tend to have harder GeV indices.

- Bottom:  $\Gamma_{\text{GeV}}$  vs. integral flux for  $E > 1 \text{ GeV}$ . For all TeV blazars,  $\Gamma_{\text{GeV}} < 2.3$  and for most of them  $\Gamma_{\text{GeV}} < 2$ , in agreement with an inverse-Compton peak frequency (IC) located in the high-energy tail of the Fermi range or beyond.



## Spectral Characteristics of GeV-TeV Blazars

Senturk et al. 2013

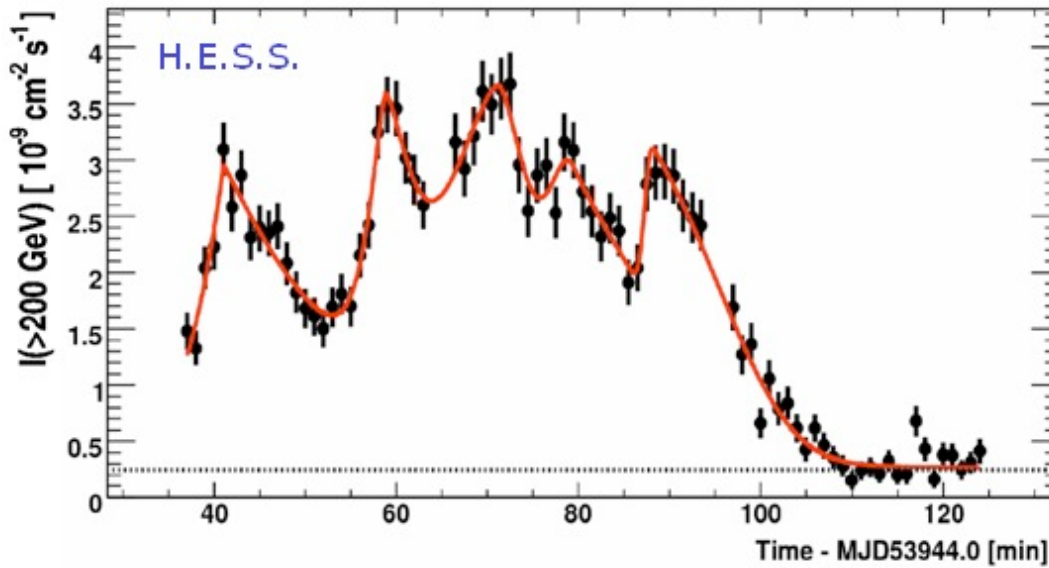


- Scatter plots of spectral indices for the Fermi-LAT bright AGN sample (LBAS) in radio-optical-Xray bands:  $\alpha_{ro}$  (5GHz – 5000 $\text{\AA}$ ),  $\alpha_{ox}$  (5000 $\text{\AA}$ – 1 keV) and  $\alpha_{x\gamma}$  (1 keV – 100MeV), comparing TeV and non-TeV sources. The TeV and non-TeV AGNs occupy separate regions in the parameter space, considering that most TeV AGNs are HBLs. [Data from \(Abdo et al. 2010a\)](#).

- Note the correlation between  $\alpha_{ro}$  and  $\alpha_{x\gamma}$ .

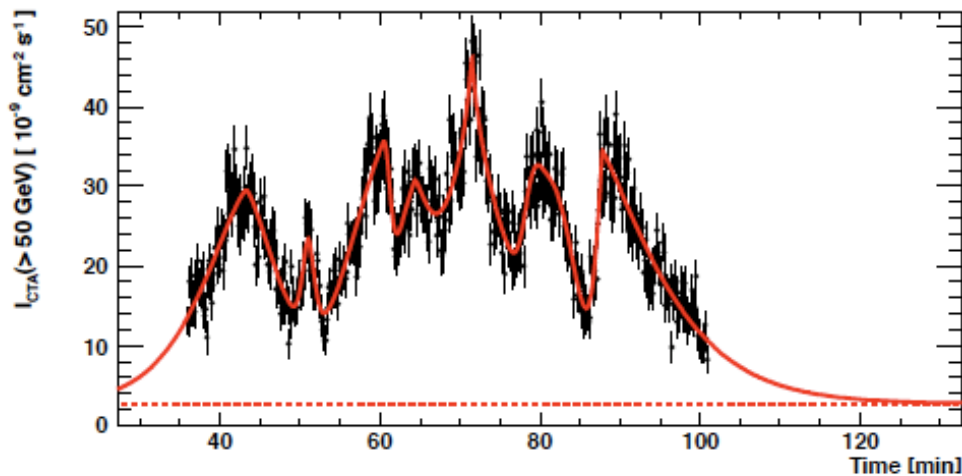
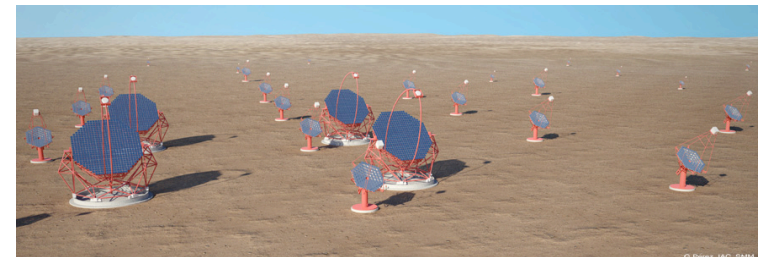
Future ...

# Future...



The big flare of PKS 2155-304 observed in 2006 by H.E.S.S., with variability down to a few minute scale.

(Aharonian et al., *Astrophys. Journal*, 664 (2007) L71)



Simulated integral flux of PKS 2155-304 above 50 GeV as CTA would monitor it. The data are binned in 7.5 seconds intervals.

(from <http://arxiv.org/pdf/1304.3024v1.pdf>)

